

# Entropic uncertainty relations for quantum information scrambling

Nicole Yunger Halpern,<sup>1, 2, \*</sup> Anthony Bartolotta,<sup>3, †</sup> and Jason Pollack<sup>4, ‡</sup>

<sup>1</sup>*Institute for Quantum Information and Matter,*

*California Institute of Technology, Pasadena, CA 91125, USA*

<sup>2</sup>*Kavli Institute for Theoretical Physics, University of California, Santa Barbara, CA 93106, USA*

<sup>3</sup>*Walter Burke Institute for Theoretical Physics, California Institute of Technology, Pasadena, CA 91125, USA*

<sup>4</sup>*Department of Physics and Astronomy, University of British Columbia, Vancouver, BC V6T 1Z1, Canada*

(Dated: June 16, 2022)

How violently do two quantum operators disagree? Different fields of physics feature different measures of incompatibility: (i) In quantum information theory, entropic uncertainty relations constrain measurement outcomes. (ii) In condensed matter and high-energy physics, the out-of-time-ordered correlator (OTOC) signals scrambling, the spread of information through many-body entanglement. We unite these measures, proving entropic uncertainty relations for scrambling. The entropies are of distributions over weak and strong measurements' possible outcomes. The weak measurements ensure that the OTOC quasiprobability (a nonclassical generalization of a probability, which coarse-grains to the OTOC) governs terms in the uncertainty bound. The quasiprobability causes scrambling to strengthen the bound in numerical simulations of a spin chain. This strengthening shows that entropic uncertainty relations can reflect the type of operator disagreement behind scrambling. Generalizing beyond scrambling, we prove entropic uncertainty relations satisfied by commonly performed weak-measurement experiments. We unveil a physical significance of weak values (conditioned expectation values): as governing terms in entropic uncertainty bounds.

## I. INTRODUCTION

How incompatible are two quantum operators,  $\hat{V}$  and  $\hat{W}(t)$ ? Two species of quantum physicist answer with two different measures. Today's pure quantum information (QI) theorist checks uncertainty relations cast in terms of entropies [1–16]. The greater the uncertainty bounds, the worse the operators' disagreement.

The second species—the condensed-matter or high-energy physicist—studies the following setup: Consider a strongly coupled quantum many-body system. Examples include an interacting spin chain and the boundary dual of a gravitational theory. The Hamiltonian,  $\hat{H}$ , couples the subsystems and generates the time-evolution operator  $\hat{U} := e^{-i\hat{H}t}$ . Let  $\hat{V}$  and  $\hat{W}$  denote Hermitian and/or unitary operators localized on far-apart subsystems. Examples include Pauli operators acting on opposite sides of the spin chain. In the Heisenberg picture, the interactions delocalize  $\hat{W}$  to  $\hat{W}(t) := \hat{U}^\dagger \hat{W} \hat{U}$ . The support of  $\hat{W}(t)$  comes to overlap the support of  $\hat{V}$ ; the operators cease to agree. The *out-of-time-ordered correlator* (OTOC) quantifies this disagreement, as well as quantum chaos and scrambling [17–34]. QI *scrambles* upon spreading across a system via many-body entanglement.

Entropic uncertainty relations and OTOCs occupy disparate subfields, but both quantify operator disagreement. We unite these quantifications, proving entropic uncertainty relations for QI scrambling (Theorem 1).

These relations make precise the extent to which scrambling drives operators away from compatibility. We then evaluate the uncertainty relations in numerical simulations of nonintegrable spin chains. The uncertainty bounds tighten when the system scrambles. Hence entropic uncertainty relations can reflect the type of operator incompatibility behind scrambling. The bounds tighten because they contain the quasiprobability behind the OTOC [35–37]. *Quasiprobabilities* resemble probabilities but can behave nonclassically, assuming negative and nonreal values. The OTOC has been shown to equal an average over a quasiprobability distribution. Recent studies have uncovered several theoretical and experimental applications of the OTOC quasiprobability [35–37]: The quasiprobability enables the OTOC to feature in a fluctuation-like relation, a generalization of the second law of thermodynamics; motivates a scheme for measuring the OTOC experimentally; distinguishes scrambling from decoherence in measurements of open-system OTOCs; and has information-theoretic applications, such as to Bayesian updating. We present a new application: The quasiprobability enables entropic uncertainty relations to reflect the same operator disagreement as the OTOC. Our entropic uncertainty relations generalize in two ways. First, they extend from the famous four-point OTOC to arbitrarily high-order, arbitrarily out-of-time-ordered correlators. Such OTOCs reflect later, subtler stages of scrambling and equilibration [36, 38–42]. Second, our entropic uncertainty relations generalize beyond many-body systems that scramble. Quasiprobabilities govern weak measurements, which barely disturb the measured system [43], similarly to how probabilities govern strong measurements. Averaging a common quasiprobability yields a *weak value*, a conditioned expectation value. Weak values' physical significances have

\* Current address and email: Harvard-Smithsonian ITAMP, 60 Garden St., MS 14, Cambridge, MA 02138, USA, nico.leyh@g.harvard.edu

† abartolo@theory.caltech.edu

‡ jpollack@phas.ubc.ca

been debated [44, 45]. We present a new physical significance: Weak values, as well as quasiprobabilities, govern first-order-in-the-weak-coupling terms in entropic uncertainty bounds (Theorem 2). These bounds govern weak-measurement experiments undertaken routinely.

## II. RESULTS

We briefly overview entropic uncertainty relations and OTOCs in Sections II A and II B. In Sec. II C, we reason intuitively to the form that entropic uncertainty relations for scrambling should assume. This intuition is then made rigorous. The setup is concretized in Sec. II D, and the measurements are formalized in Sec. II E. The POVMs' possible outcomes obey probability distributions whose entropies we define in Sec. II F. We present in Sec. II G, and analyze in Sec. II H, the entropic uncertainty relations for scrambling. Numerical simulations of a spin chain illustrate the results in Sec. II I. We generalize to higher-point OTOCs in Sec. II J, then to weak values beyond scrambling in Sec. II K.

### II A. Entropic uncertainty relations

Heisenberg captured the complementarity of position and momentum in [46]. Kennard concretized this complementarity in the first uncertainty relation [47]. Robertson proved the uncertainty relation featured in many textbooks [48]:

$$\Delta\hat{A}\Delta\hat{B} \geq \frac{1}{2} |\langle[\hat{A}, \hat{B}]\rangle|. \quad (1)$$

We have set  $\hbar$  to one.  $\hat{A}$  and  $\hat{B}$  denote observables defined on a Hilbert space  $\mathcal{H}$ . The expectation value  $\langle \cdot \rangle$  is evaluated on a state  $|\psi\rangle \in \mathcal{H}$ . The standard deviation  $\Delta\hat{A} := \sqrt{\langle\hat{A}^2\rangle - \langle\hat{A}\rangle^2}$  quantifies the spread in the possible outcomes of a measurement of  $\hat{A}$ .

The standard deviations have provoked objections (e.g., [5]). For example, consider relabeling the eigenvalues  $a$  of  $\hat{A}$ . Relabeling should not change the operators' compatibility, but  $\Delta\hat{A}$  can skyrocket. Stripping the  $a$ 's off of  $\Delta\hat{A}$  leaves a function of probabilities: Denote by  $p_a$  the probability that a measurement of  $\hat{A}$  yields  $a$ . On probability distributions  $\{p_a\}$  are defined entropies. Entropies, the workhorses of information theory, quantify the optimal rates at which information-theoretic and thermodynamic tasks can be performed [49–52]. Entropies replace standard deviations in modern uncertainty relations [1–16].

The *Maassen-Uffink relation* exemplifies entropic uncertainty relations [7]:

$$H(\hat{A}) + H(\hat{B}) \geq -\log c. \quad (2)$$

The Shannon entropy is defined as  $H(\hat{A}) := -\sum_a p_a \log p_a$ . The *maximum overlap*  $c$  is defined in terms of the eigendecompositions

$$\hat{A} = \sum_a a|a\rangle\langle a| \quad \text{and} \quad \hat{B} = \sum_b b|b\rangle\langle b| \quad (3)$$

as

$$c := \max_{a,b} |\langle a|b\rangle|^2. \quad (4)$$

Hence the bound (2) is independent of the eigenvalues  $a$ , as desired. The bound is tight if  $c$  is small.  $c$  is smallest when the eigenbases are *mutually unbiased*:  $|\langle a|b\rangle| = \frac{1}{\sqrt{d}}$ , wherein  $d := \dim(\mathcal{H})$  denotes the Hilbert space's dimensionality. For example, the Pauli operators  $\hat{\sigma}^x$  and  $\hat{\sigma}^z$  have mutually unbiased eigenbases. If you prepare any eigenstate of  $\hat{\sigma}^x$ , then measure  $\hat{\sigma}^z$ , you have no idea which outcome will obtain. Hence  $\hat{\sigma}^x$  and  $\hat{\sigma}^z$  are said to fail *maximally* to commute. Entropic uncertainty relations have applications to many topics in quantum theory, including quantum correlations, steering, coherence, and wave-particle duality (see [15] and references therein).

### II B. Out-of-time-ordered correlators

OTOCs reflect chaos and QI spreading in quantum many-body systems. Settings range from ultracold atoms and trapped ions to holographic black holes (e.g., [17–34, 53]). Let  $\mathcal{H}$  denote a quantum many-body system's Hilbert space. Let  $\hat{\rho} \in \mathcal{D}(\mathcal{H})$  denote an arbitrary state of the system.  $\mathcal{D}(\mathcal{H})$  denotes the space of density operators, or trace-one positive-semidefinite linear operators, defined on  $\mathcal{H}$ . The OTOC has the form

$$F(t) := \left\langle \hat{W}^\dagger(t) \hat{V}^\dagger \hat{W}(t) \hat{V} \right\rangle \equiv \text{Tr} \left( \hat{W}^\dagger(t) \hat{V}^\dagger \hat{W}(t) \hat{V} \hat{\rho} \right), \quad (5)$$

for unitary and/or Hermitian  $\hat{V}$  and  $\hat{W}$  localized far apart. The OTOC forms the nontrivial component of

$$\left\langle |[\hat{W}(t), \hat{V}]|^2 \right\rangle. \quad (6)$$

This magnitude-squared commutator equals  $2[1 - F(t)]$  if  $\hat{V}$  and  $\hat{W}$  are unitary (e.g., Pauli operators).

Several pieces of evidence imply that the OTOC signals chaos. We review a semiclassical argument about the butterfly effect: Classical chaos hinges on sensitivity to initial perturbations. Consider initializing a classical double pendulum at a phase-space point  $\mathbf{P}$  with a strong kick. Let the pendulum begin another trial at a nearby point  $\mathbf{P} + \boldsymbol{\varepsilon}$ . The pendulum follows different phase-space trajectories in the two trials. The trajectories diverge exponentially, as quantified with a Lyapunov exponent  $\lambda_L$ .

The OTOC captures a similar divergence. Let us construct two protocols that differ largely by an initial perturbation. The system could consist of an  $N$ -site chain

of spin- $\frac{1}{2}$  degrees of freedom, or *qubits*. Suppose that  $\hat{\rho} = |\psi\rangle\langle\psi|$  is pure. Protocol I consists of (i) preparing the system in  $|\psi\rangle$ , (ii) perturbing the system with a local  $\hat{V}$  (as by flipping spin 1 with  $\hat{\sigma}_1^x$ ), (iii) evolving the system under a nonintegrable Hamiltonian, (iv) perturbing with a local  $\hat{W}$  (such as the final spin's  $\hat{\sigma}_N^z$ ), and (v) evolving the system backward, under  $\hat{U}^\dagger$ . This protocol prepares  $|\psi_1\rangle := \hat{W}(t)\hat{V}|\psi\rangle$ .

Following protocol II, one prepares  $|\psi\rangle$  and skips the initial  $\hat{V}$ . The system evolves forward under  $\hat{U}$ , is perturbed with  $\hat{W}$ , and reverse-evolves under  $\hat{U}^\dagger$ . Only afterward does  $\hat{V}$  perturb the system. Protocol II prepares  $|\psi_{II}\rangle := \hat{V}\hat{W}(t)|\psi\rangle$ .

How much does the initial  $\hat{V}$  perturbation affect the system's final state? The answer manifests in the overlap

$$|\langle\psi_{II}|\psi_1\rangle| = |F(t)| \sim 1 - \frac{e^{\lambda t}}{N}. \quad (7)$$

Nonlocal systems, such as the Sachdev-Ye-Kitaev (SYK) model [19, 28, 54, 55], obey the final relation. [In local systems,  $F(t)$  decays polynomially.] The relation holds during a time window around the *scrambling time*,  $t_*$ . The Lyapunov-type exponent  $\lambda$  controls the exponential decay. Hence  $F(t)$  reflects a Lyapunov-type divergence reminiscent of classical-chaotic sensitivity to initial perturbations.

Smallness of  $F(t)$  tends to reflect highly nonlocal entanglement. After  $t_*$ , no local probe  $\hat{V}$  can recover information about any earlier, initially local perturbation  $\hat{W}$ . This many-body nonlocality is called *scrambling* [26, 56].

### II C. Intuitive construction of entropic uncertainty relations for scrambling

Uncertainty relations and OTOCs, reflecting quantum operator disagreement in different subfields, cry out for unification. But how can one form an uncertainty relation for scrambling? One might try substituting  $\hat{A} = \hat{V}$  and  $\hat{B} = \hat{W}(t)$  into the uncertainty relation (2). But the bound would bear no signature of scrambling. Moreover, simulations imply, simple choices of  $\hat{V}$  and  $\hat{W}(t)$  eigenbases fail to become mutually unbiased after  $t_*$  [36].

A clue suggests how entropic uncertainty relations for scrambling may be realized: The entropic inequality (2) replaced the textbook inequality (1). Inequality (1) contains one commutator. The OTOC appears in a commutator's squared magnitude [Eqs. (5) and (6)]. Hence “squaring” Ineq. (2), in some sense, might yield an entropic uncertainty relation for scrambling.

How might this “squaring” manifest? In the left-hand side (LHS) of Ineq. (2), each entropy  $H$  depends on one operator,  $\hat{A}$  or  $\hat{B}$ . Imagine “doubling” each operator by replacing it with two operators. The two operators suited to scrambling are  $\hat{V}$  and  $\hat{W}(t)$ . We therefore envision an entropy  $H(\hat{V}\hat{W}(t))$  defined in terms of a measurement of  $\hat{V}$  followed by a measurement of  $\hat{W}(t)$ . This replacement

for  $H(\hat{A})$  must differ from the replacement for  $H(\hat{B})$ , but the OTOC contains only two local operators. We therefore reverse the measurements:  $H(\hat{B}) \rightarrow H(\hat{W}(t)\hat{V})$ . The reversal mirrors the OTOC's semiclassical interpretation, Eq. (7).

How can the right-hand side (RHS) of Ineq. (2) be “squared”?  $c$  equals a product of two inner products. “Squaring”  $c$  creates a product of four inner products, or the trace of four outer products  $|\dots\rangle\langle\dots|$ . Outer products generalize to projectors  $\Pi$ . Hence a trace of a product of four projectors,  $\text{Tr}(\Pi\Pi\Pi\Pi)$ , should appear in an entropic uncertainty bound for scrambling. Such a trace is known to characterize scrambling. It forms the *quasiprobability behind the OTOC* [35–37].

Quasiprobability distributions represent quantum states as probability distributions represent classical statistical-mechanical states. Like probabilities, quasiprobabilities are normalized to one. Yet quasiprobabilities violate axioms of probability theory, such as nonnegativity and reality. Such nonclassical behaviors can signal nonclassical physics, such as the capacity for superclassical computation [57–60].

The OTOC equals an average over a quasiprobability distribution defined as follows [35, 36]. The OTOC operators eigendecompose as

$$\hat{V} = \sum_{v_\ell} v_\ell \hat{\Pi}_{v_\ell}^{\hat{V}} \quad \text{and} \quad \hat{W}(t) = \sum_{w_m} w_m \hat{\Pi}_{w_m}^{\hat{W}(t)}. \quad (8)$$

In the spin-chain example, the eigenvalues  $v_\ell, w_m = \pm 1$ . The projector  $\hat{\Pi}_{v_\ell}^{\hat{V}}$  projects onto the eigenvalue- $v_\ell$  eigenspace of  $\hat{V}$ .  $\hat{\Pi}_{w_m}^{\hat{W}(t)}$  is defined analogously. Consider substituting from Eqs. (8) into the OTOC definition (5). Factoring out the sums and the eigenvalues yields<sup>1</sup>

$$F(t) = \sum_{v_1, w_1, v_2, w_2} v_1 w_1 v_2^* w_2^* \tilde{\mathcal{A}}_{\hat{\rho}}(v_1, w_1, v_2, w_2). \quad (9)$$

The OTOC equals an average over the OTOC quasiprobability,

$$\tilde{\mathcal{A}}_{\hat{\rho}}(v_1, w_1, v_2, w_2) := \text{Tr} \left( \hat{\Pi}_{w_2}^{\hat{W}(t)} \hat{\Pi}_{v_2}^{\hat{V}} \hat{\Pi}_{w_1}^{\hat{W}(t)} \hat{\Pi}_{v_1}^{\hat{V}} \hat{\rho} \right). \quad (10)$$

The quasiprobability forms a distribution  $\{\tilde{\mathcal{A}}_{\hat{\rho}}\}$ . This set of numbers contains more information than the OTOC, which follows from coarse-graining.  $\tilde{\mathcal{A}}_{\hat{\rho}}$  concretizes the relationship between scrambling and nonequilibrium statistical mechanics, informs a scheme for measuring the OTOC experimentally, and distinguishes scrambling from decoherence in measurements of open-system OTOCs [35–37]. This paper presents a new application of the OTOC quasiprobability:  $\tilde{\mathcal{A}}_1$  governs terms in the entropic uncertainty bound for scrambling.

<sup>1</sup> The index list  $(v_1, w_1, v_2, w_2)$  here is equivalent to the index list  $(v_1, w_2, v_2, w_3)$  in [35, 36].

The quasiprobability tightens the bound when the system scrambles. We evaluate the quasiprobability on the identity operator  $\hat{\mathbb{1}}$  because entropic uncertainty bounds cannot depend on any state  $\hat{\rho}$ . Uncertainty relations require, moreover, that eigenvalues be “stripped off” of operators.  $\tilde{\mathcal{A}}_{\hat{\mathbb{1}}}$  follows from stripping the eigenvalues off the OTOC, by Eq. (9).

We can predict the form of the uncertainty-bound term that will contain  $\tilde{\mathcal{A}}_{\hat{\mathbb{1}}}$ . Quasiprobabilities can be measured via weak measurement: An interaction Hamiltonian couples a detector to the system. A small coupling constant  $g$  governs the interaction. The measurement disturbs the measured state at high order in  $g$ . From weak and strong measurements of  $\hat{V}$  and  $\hat{W}(t)$ , the OTOC quasiprobability can be inferred experimentally [35, 36, 41].  $\tilde{\mathcal{A}}_{\hat{\rho}}$  is extracted from the data through a high-order term.  $\tilde{\mathcal{A}}_{\hat{\mathbb{1}}}$  should therefore appear in a high-order-in- $g$  term in our entropic uncertainty bound.

The uncertainty relation’s RHS contains  $g$  only if the LHS involves weak measurements. Consider measuring  $\hat{V}$  weakly, then  $\hat{W}(t)$  strongly. Each possible pair  $(v_\ell, w_m)$  of outcomes has some probability of obtaining. On this probability, we propose to define the entropy  $H(\hat{V}\hat{W}(t))$ .  $H(\hat{W}(t)\hat{V})$  should be defined similarly.

Let us summarize our intuitive reasoning. Entropic uncertainty relations for scrambling should have the form

$$H(\hat{V}\hat{W}(t)) + H(\hat{W}(t)\hat{V}) \geq g^{k-1}(\text{classical factor}) + g^k(\text{const.})\tilde{\mathcal{A}}_{\hat{\mathbb{1}}}(v_1, w_1, v_2, w_2) + O(g^{k+1}). \quad (11)$$

The exponent  $k \geq 2$ .  $H(\hat{V}\hat{W}(t))$  quantifies the uncertainty about the outcomes that follow from preparing an arbitrary  $\hat{\rho}$ , measuring  $\hat{V}$  weakly, and then measuring  $\hat{W}(t)$  strongly.  $H(\hat{W}(t)\hat{V})$  results from reversing the measurement protocol. Having constructed expectations via intuition, we now prove them.

## II D. Setup

We continue to focus on a quantum many-body system illustrated with a chain of  $N$  qubits. To simplify notation, we omit hats from operators. Many-body quantities are defined as in the introduction: the Hilbert space  $\mathcal{H}$ , its dimensionality  $d$ , the arbitrary state  $\rho \in \mathcal{D}(\mathcal{H})$ , the Hamiltonian  $H$ , the time-evolution unitary  $U$ , the local operators  $V$  and  $W$  (illustrated with  $\sigma_1^z$  and  $\sigma_N^z$ ), the Heisenberg-picture  $W(t)$ , the projectors  $\Pi_{v_\ell}^V$  and  $\Pi_{w_m}^{W(t)}$ , the eigenvalues  $v_\ell$  and  $w_m$ , the OTOC  $F(t)$ , and the OTOC quasiprobability  $\tilde{\mathcal{A}}_{\hat{\rho}}$ .

The Hilbert space  $\mathcal{H}$  is assumed to be discrete, in accordance with [14, 61], whose results we use. Continuous-variable systems are addressed in the “outlook” (Sec. III). We emphasize nonintegrable, nonlocal Hamiltonians. We assume that  $V$  and  $W$  are Hermitian, for simplicity, but the results generalize: Each of  $V$  and  $W$  can be Hermitian and/or unitary [35, 36]. If  $V$  is unitary but not

Hermitian, for example, measurements of  $V$  are replaced with measurements of the Hermitian generator of  $V$ .

## II E. Formalization of measurements

A sequence of  $V$  and  $W(t)$  measurements forms a generalized measurement. Generalized measurements are formalized, in QI theory, with *positive operator-valued measures* (POVMs) [50]. A POVM  $\{M_x\}$  consists of positive operators  $M_x > 0$  that obey the completeness condition  $\sum_x M_x^\dagger M_x = \mathbb{1}$ .  $x$  labels the outcomes.

POVMs replace measurements of observables  $A$  and  $B$  in generalized entropic uncertainty relations [14, 61]. We adapt the formalism used by Tomamichel [14], for concreteness and for ease of comparison with a standard reference. In [14] appear POVMs illustrated with measurements of observables.

These general POVMs manifest, in the context of scrambling, as follows. We label as “the forward measurement” a weak measurement of  $V$ , followed by a projective measurement of  $W(t)$ . We use the term “weak measurement of  $V$ ” as in [36]: A projector  $\Pi_{v_1}^V$  is effectively measured weakly. One can effectively measure a qubit system’s  $\Pi_{v_1}^V$  by, e.g., coupling the detector to  $V$  and calibrating the detector appropriately. The experimenter chooses the value of  $v_1$ ; the choice directs the calibration. See Sec. II I 1 and [36, Sec. I D 4] for example implementations. The reverse process constitutes the second POVM, for a definition of “reverse” that we concretize after formalizing the weak measurement.

To measure  $\Pi_{v_\ell}^V$  weakly, one prepares a detector in a state  $|D\rangle$ . The system’s  $\Pi_{v_\ell}^V$  is coupled weakly to a detector observable, via an interaction unitary  $V_{\text{int}}$ . A detector observable is measured projectively, yielding an outcome  $j_\ell$ .

The weak measurement induces dynamics modeled with *Kraus operators* [50, 62]. Kraus operators represent the system-of-interest evolution effected by a coupling to an ancilla, which effectively measures the system:

$$K_{j_\ell}^{V,v_\ell} = \langle j_\ell | V_{\text{int}} | D \rangle = \sqrt{p_{j_\ell}^V} \mathbb{1} + g_{j_\ell}^V \Pi_{v_\ell}^V. \quad (12)$$

The operators satisfy the completeness relation  $\sum_{j_\ell} (K_{j_\ell}^{V,v_\ell})^\dagger K_{j_\ell}^{V,v_\ell} = \mathbb{1}$ . Let  $\rho$  temporarily denote the system’s precoupling state. The detector has a probability  $\text{Tr}(K_{j_\ell}^{V,v_\ell} \rho [K_{j_\ell}^{V,v_\ell}]^\dagger)$  of registering the outcome  $j_\ell$ . The outcome-dependent  $g_{j_\ell}^V \in \mathbb{C}$  quantifies the interaction strength. The experimenter can tune  $g_{j_\ell}^V$ , whose smallness reflects the measurement’s weakness:  $|g_{j_\ell}^V| \ll 1$ . We refer to various constants  $g_{j_\ell}^V$  as  $g$ ’s.

Imagine strongly measuring the detector observable without having coupled the detector to the system. The outcome  $j_\ell$  has a probability  $p_{j_\ell}^V$  of obtaining. We invoke Kraus operators’ unitary equivalence [62] to ensure that  $p_{j_\ell}^V \in \mathbb{R}$ .

The forward POVM  $\{M_{j_1, w_1}^{F, v_1}\}$  is defined through the composite Kraus operators

$$\sqrt{M_{j_1, w_1}^{F, v_1}} := \Pi_{w_1}^{W(t)} K_{j_1}^{V, v_1}. \quad (13)$$

Recall that  $\Pi_{w_1}^{W(t)}$  projects onto the  $w_1$  eigenspace of  $W(t)$ . Each POVM element has the form  $\left(\sqrt{M_{j_1, w_1}^{F, v_1}}\right)^\dagger \sqrt{M_{j_1, w_1}^{F, v_1}}$ .

The reverse POVM,  $\{M_{j_2, w_2}^{R, v_2}\}$ , is defined through the composite Kraus operators<sup>2</sup>

$$\sqrt{M_{j_2, w_2}^{R, v_2}} := \left(\Pi_{w_2}^{W(t)} K_{j_2}^{V, v_2}\right)^\dagger = \left(K_{j_2}^{V, v_2}\right)^\dagger \Pi_{w_2}^{W(t)}. \quad (14)$$

To round out the reversal, we not only swap the  $V$  measurement with the  $W(t)$ , but also Hermitian-conjugate. Conjugation negates imaginary numbers. It represents, e.g., the time-reversal of magnetic fields.

Let us clarify which variables are chosen and which vary randomly.  $w_1$  is a random outcome whose value varies from realization to realization of the forward POVM.  $w_2$  is a random outcome whose value varies from realization to realization of the reverse POVM. The experimentalist chooses the values of  $v_1$  and  $v_2$ . Though a forward trial's  $v_1$  and  $w_1$  can differ from a reverse trial's  $v_2$  and  $w_2$ , both protocols' measurements [of  $V$  and of  $W(t)$ ] are essentially the same.

## II F. Entropies

Consider preparing the system in the state  $\rho$ , then measuring the forward POVM,  $\{M_{j_1, w_1}^{F, v_1}\}$ . One prepares a detector in some fiducial state. Some detector observable is effectively coupled to the system's  $\Pi_{v_1}^V$ . Then, some detector observable couples to a classical<sup>3</sup> register. The register records an outcome  $j_1$ . Next, the system's  $W(t)$  couples to another classical register. This register records the outcome  $w_1$ .

The two-register system ends in the state

$$\rho_F := \sum_{j_1, w_1} \text{Tr} \left( \sqrt{M_{j_1, w_1}^{F, v_1}} \rho \sqrt{M_{j_1, w_1}^{F, v_1}}^\dagger \right) |j_1\rangle\langle j_1| \otimes |w_1\rangle\langle w_1|. \quad (15)$$

The eigenvalues,  $\text{Tr} \left( \sqrt{M_{j_1, w_1}^{F, v_1}} \rho \sqrt{M_{j_1, w_1}^{F, v_1}}^\dagger \right)$ , form a probability distribution over the possible pairs  $(j_1, w_1)$  of mea-

surement outcomes. Entropies of the distribution equal entropies of  $\rho_F$ .<sup>4</sup>

The order- $\alpha$  Rényi entropy of a quantum state  $\sigma$  is

$$H_\alpha(\sigma) := \frac{1}{1-\alpha} \log(\text{Tr}(\sigma^\alpha)). \quad (16)$$

We choose for all logarithms to be base-2, following [14]. The von Neumann entropy is

$$H_{\text{vN}}(\sigma) = \lim_{\alpha \rightarrow 1} H_\alpha(\sigma) = -\text{Tr}(\sigma \log \sigma). \quad (17)$$

The *min entropy* is defined as

$$H_{\min}(\sigma) := H_\infty(\sigma) := \lim_{\alpha \rightarrow \infty} H_\alpha(\sigma) \quad (18)$$

$$= \sup\{\lambda \in \mathbb{R} : \sigma \leq 2^{-\lambda} \mathbb{1}\} \quad (19)$$

$$= -\log(p_{\max}). \quad (20)$$

$p_{\max}$  denotes the greatest eigenvalue of  $\sigma$ .

The *max entropy* is

$$H_{\max}(\sigma) := H_{1/2}(\sigma) = \log(\|\sqrt{\sigma}\|_1^2). \quad (21)$$

The Schatten 1-norm is denoted by  $\|\cdot\|_1$ . The general Schatten  $p$ -norm of a Hermitian operator  $\sigma = \sum_j s_j |s_j\rangle\langle s_j|$  is

$$\|\sigma\|_p = [\text{Tr}(\sigma^p)]^{1/p} = \left( \sum_j |s_j|^p \right)^{1/p}, \quad (22)$$

for  $p \geq 1$  [63].  $H_{\max}$  reflects the discrepancy between  $\sigma$  and the maximally mixed state [14, p. 60]: The fidelity between normalized states  $\sigma$  and  $\gamma$  is<sup>5</sup>  $F(\sigma, \gamma) := \|\sqrt{\sigma} \sqrt{\gamma}\|_1$ .  $H_{\max}$  depends on the fidelity through:  $H_{\max}(\sigma) = \log(d[F(\sigma, \mathbb{1}/d)]^2)$ .

We note the detector state's Rényi entropies as

$$H_\alpha(VW(t))_\rho := H_\alpha(\rho_F), \quad (23)$$

following [14]. We have now introduced the forward-POVM entropies. The two-detector state  $\rho_R$ , and the entropy  $H_\alpha(W(t)V)$ , are defined analogously.

$H_{\max}$  and  $H_{\min}$ , like  $H_{\text{vN}}$ , quantify rates at which information-processing and thermodynamic tasks can be performed. Applications include quantum key distribution, randomness extraction, erasure, work extraction, and work expenditure (e.g., [14, 51, 64–69]). Quantum states desired for such tasks cannot be prepared exactly. *Smoothing* introduces an error tolerance  $\varepsilon \in [0, 1)$  into the entropies [64]. Our uncertainty relations for scrambling generalize to smooth entropies. We focus on non-smooth entropies for simplicity.

<sup>2</sup> Ending the protocol with a weak measurement might disconcert measurement theorists. But this reverse protocol captures the OTOC's forward-and-reverse spirit [Eq. (7)], as explained earlier.

<sup>3</sup> “Classical” means, here, that the register can occupy only quantum states representable by density matrices diagonal with respect to a fixed basis.

<sup>4</sup> In defining the entropies, we mostly follow Tomamichel's conventions [14]. Yet we assume that all states  $\sigma$  are normalized:  $\text{Tr}(\sigma) = 1$ .

<sup>5</sup> Tomamichel uses the generalized fidelity. When we evaluate the generalized fidelity, at least one argument is normalized. The generalized fidelity therefore simplifies to the fidelity [14, p. 48].

## II G. Entropic uncertainty relations for QI scrambling

We can now reconcile the two notions of quantum operator disagreement, entropic uncertainty relations of pure QI theory and information scrambling of high-energy and condensed-matter theory.

**Theorem 1.** *The forward and reverse POVMs satisfy entropic uncertainty relations for scrambling,*

$$H_{\text{vN}}(VW(t))_\rho + H_{\text{vN}}(W(t)V)_\rho \geq f(v_1, v_2) \text{ and} \quad (24)$$

$$H_\alpha(VW(t))_\rho + H_\beta(W(t)V)_\rho \geq f(v_1, v_2), \quad (25)$$

for  $\varepsilon \geq 0$ . The bound depends on the OTOC quasiprobability:

$$\begin{aligned} f(v_1, v_2) := \min_{j_1, j_2, w_1, w_2} & \left\{ C_0 + \text{Re}(g_{j_1}^V) C_1 + \text{Re}(g_{j_2}^V) C'_1 \right. \\ & + \text{Re}\left(g_{j_1}^V g_{j_2}^V \tilde{\mathcal{A}}_1(v_1, w_1, v_2, w_2)\right) C_2 \quad (26) \\ & + |g_{j_1}^V|^2 \tilde{\mathcal{A}}_1(v_1, w_1, v_1, w_2) C'_2 \\ & \left. + |g_{j_2}^V|^2 \tilde{\mathcal{A}}_1(v_2, w_1, v_2, w_2) C''_2 + O(g^2) \right\}. \end{aligned}$$

The real numbers  $C$ , and the rest of the  $\sim g^2$  terms, depend essentially on classical probabilities. Their forms are given below.

The  $j$  and  $w$  dependences of the  $C$ 's have been suppressed for conciseness. Inequality (25) can be smoothed when  $(\alpha, \beta) = (\infty, 1/2)$ .

The uncertainty relations are proved in App. A. They follow from three general uncertainty relations: Result 7 in [14], Corollary 2.6 in [61], and Ineq. (13) in [70]. The OTOC POVMs (13) and (14) are substituted into the general uncertainty relations. The POVMs' maximum overlap,  $c$ , cannot obviously be inferred from parameters chosen, or from measurements taken, in an OTOC-inference experiment. We therefore bound  $c$ , using  $\tilde{\mathcal{A}}$  and the Schatten  $p$ -norm's monotonicity in  $p$ :

$$\begin{aligned} -\log c \geq \log \left( \min_{j_1, j_2, w_1, w_2} \left\{ \right. \right. \quad (27) \\ \left. \left. \text{Tr} \left( \Pi_{w_2}^{W(t)} K_{j_2}^{V, v_2} \left[ K_{j_1}^{V, v_1} \right]^\dagger \Pi_{w_1}^{W(t)} K_{j_1}^{V, v_1} \left[ K_{j_2}^{V, v_2} \right]^\dagger \right) \right\} \right). \end{aligned}$$

We substitute in for the  $K$ 's from Eq. (12), then multiply out. In each of several terms, two  $K$ 's contribute  $\Pi_{v_\ell}^V$ 's, while two  $K$ 's contribute  $\mathbb{1}$ 's. These terms contain quasiprobability values  $\tilde{\mathcal{A}}_1$ . We isolate the terms by Taylor-expanding the logarithm in the  $g$ 's.

## II H. Analysis

Four points merit analysis: the POVMs' implications for the butterfly effect, the form of the bound  $f(v_1, v_2)$ ,

simple limits, and conditions that render the bound non-trivial.

**Implications for the butterfly effect:** The weak measurements strengthen an analogy between the OTOC and the butterfly effect of classical chaos [20, 29, 30, 71]. In the classical butterfly effect, a tiny perturbation snowballs into a drastic change. This perturbation has been likened to operation by a unitary  $V$ , in Eq. (7).  $V$  should be associated with a weak measurement, Theorem 1 clarifies. The measurement is perturbative in  $g_{j_\ell}^V$ .

**Form of the uncertainty bound  $f(v_1, v_2)$  for scrambling:** The bound (26) contains three terms dependent on the quasiprobability  $\tilde{\mathcal{A}}_1$ . These terms' proportionality to  $g^2$  accords with intuition: Scrambling is a subtle feature of quantum equilibration, detectable in just many-point correlators. Likewise, the OTOC quasiprobability governs high-order terms in the uncertainty bound. As anticipated in Sec. II, the quasiprobability  $\tilde{\mathcal{A}}_1$  is evaluated on the identity operator. The bound highlights the operator disagreement without pollution by any state  $\rho$ .

The quasiprobability-free terms in (26) are “background terms”: They contain classical probabilities, accessible without weak measurements. The  $g$ -independent term,

$$C_0 := -\log (p_{j_1}^V p_{j_2}^V \text{Tr}(\Pi_{w_2}^W \delta_{w_1 w_2})), \quad (28)$$

dominates  $f(v_1, v_2)$ . The Kronecker delta is denoted by  $\delta_{w_1 w_2}$ . The two linear terms,

$$\begin{aligned} C_1 &:= \frac{-2}{\ln 2} p(v_1|w_2) \frac{\text{Re}(g_{j_1}^V)}{\sqrt{p_{j_1}^V}} \quad \text{and} \\ C'_1 &:= \frac{-2}{\ln 2} p(v_2|w_2) \frac{\text{Re}(g_{j_2}^V)}{\sqrt{p_{j_2}^V}}, \quad (29) \end{aligned}$$

depend on projectors  $\Pi$  only through classical probabilities  $p(v_\ell|w_m) = \text{Tr}(\Pi_{v_\ell}^V \Pi_{w_m}^{W(t)}) / \text{Tr}(\Pi_{w_m}^{W(t)})$ . This  $p(v_\ell|w_m)$  equals the conditional probability that, if the system begins maximally mixed over the  $w_m$  eigenspace of  $W(t)$ , if  $V$  is measured, outcome  $v_\ell$  will obtain. Such classical dependence characterizes also the  $g^2$  terms suppressed in Eq. (26),

$$\begin{aligned} & \frac{-1}{\ln 2} p(v_1|w_2) \text{Re}\left(g_{j_1}^V [g_{j_2}^V]^*\right) \delta_{v_1 v_2} \quad (30) \\ & + \frac{2}{\text{Tr}(\Pi_{w_2}^W)} \left[ \frac{\text{Re}(g_{j_1}^V)}{\sqrt{p_{j_1}^V}} p(v_1|w_2) + \frac{\text{Re}(g_{j_2}^V)}{\sqrt{p_{j_2}^V}} p(v_2|w_2) \right]^2. \end{aligned}$$

The dominance of  $C_0$ , the  $\delta_{w_1 w_2}$  in  $C_0$ , and the min ensure that  $w_1 = w_2$  throughout the min's argument. The first  $\tilde{\mathcal{A}}_1$  has four arguments,  $(v_1, w_1, v_2, w_2)$ , constrained only by the  $\delta_{w_1 w_2}$ . In each other  $\tilde{\mathcal{A}}_1$ , the first argument must equal the third, even before the minimization is imposed. For example, the second quasiprobability value

has the form  $\tilde{\mathcal{A}}_1(v_1, w_1, v_1, w_2)$ . The  $V$  eigenvalues equal each other, due to Ineq. (27). One  $v_1$  comes from the  $(K_{j_1}^{V, v_1})^\dagger$ , and one, from the  $K_{j_1}^{V, v_1}$ .

**Nontriviality conditions:** The Rényi entropies are nonnegative:  $H_\alpha(\sigma) \geq 0$ . Hence the bound is nontrivial when positive:  $f(v_1, v_2) > 0$ . When the coupling is weak, the bound is positive when its first term is positive. The first term simplifies to  $\min_{j_1, j_2, w_2} \{-\log(p_{j_1}^V p_{j_2}^V \text{Tr}(\Pi_{w_2}^W))\}$ . The trace is large in the system size, equaling  $2^{N-1}$  in the spin-chain example. One might worry that this trace swells the log, drawing the bound far below zero.

The probabilities  $p_{j_\ell}^V$  can offset the enormity. Let us focus on the spin-chain example and approximate  $p_{j_1}^V \approx p_{j_2}^V \equiv p_{j_\ell}^V$ . Nonnegativity of the log term becomes equivalent to  $(p_{j_\ell}^V)^2 2^{N-1} \leq 1$ , or  $p_{j_\ell}^V \leq \frac{1}{2^{(N-1)/2}}$ . Strongly measuring a weak-measurement detector must yield one of  $\geq 2^{(N-1)/2}$  possible outcomes.

Weak measurements as in [44] satisfy this requirement. Let each detector manifest as a particle, e.g., in a potential that defines a dial. Let  $O$  denote the strongly measured detector observable (e.g., the position  $\hat{x}$ ). Let  $\tilde{O}$  denote the conjugate observable (e.g., the momentum  $\hat{p}$ ):  $[O, \tilde{O}] = \pm i\hbar$ . Let be prepared in a Gaussian state that peaks sharply at some  $\tilde{O}$  eigenvalue (e.g., a sharp momentum-space wave packet). The probabilities  $p_{j_\ell}^V$  can be small enough that  $f(v_1, v_2) > 0$ . We present an example in Sec. II I.

The  $g$ -free log encodes randomness in a measurement of a detector that has never coupled to the system. Hence the log fails to reflect disagreement between  $V$  and  $W(t)$ . The disagreement manifests in the  $g$ -dependent terms.

**Simple limits:** Three simple limits illuminate the bound's behavior: early times ( $t \approx 0$ ), late times ( $t \geq t_*$ ), and the weak limit ( $g \rightarrow 0$ ). We focus on a chaotic spin chain, for concreteness. Numerical simulations (Sec. II I) support these arguments.

*Early times* ( $t \approx 0$ ):  $V$  and  $W(t) \approx W$  nontrivially transform just far-apart subsystems. Hence  $\text{Tr}(\Pi_{w_\ell}^{W(t)} \Pi_{v_m}^V) \approx 2^{N-2}$ . Also,  $[V, W(t)] \approx 0$ , so the projectors nearly commute. Hence  $\text{Tr}(\Pi_{w_\ell}^{W(t)} \Pi_{v_m}^V \Pi_{w_{\ell'}}^{W(t)} \Pi_{v_{m'}}^V) \approx 2^{N-2} \delta_{w_\ell w_{\ell'}} \delta_{v_m v_{m'}}$ . These traces are large, dragging the  $\sim g$  terms in Eq. (26), and the negative term in (30), below zero. The  $g$ 's mitigate the dragging's magnitude. Still, the bound is expected to be relatively loose before  $t_*$ .

*Late times* ( $t \geq t_*$ ):  $V$  can fail to commute with  $W(t)$ . Traces  $\text{Tr}(\Pi_{w_\ell}^{W(t)} \Pi_{v_m}^V \dots)$  will shrink: Consider a one-qubit system, as a simple illustration. Suppose that  $V = \sigma^z$  and that  $W = \sigma^x$ . Each  $\Pi_{w_\ell}^{W(t)} \Pi_{v_m}^V$  translates roughly into a  $|\langle x_\ell | z_m \rangle|^2 = \frac{1}{d}$ . The traces' smallness tightens the uncertainty bound, as expected when the

system is scrambled (as explained in the introduction).<sup>6</sup> The bound likely does not remain at its maximum possible value at all  $t > t_*$ , however. As  $W(t)$  evolves, the bound should fluctuate around a relatively large value.

*Weak limit* ( $g \rightarrow 0$ ): The system fails to couple to the detectors. The bound (26) reduces to  $\min_{w_2} \{-\log(p_{j_1}^V p_{j_2}^V \text{Tr}(\Pi_{w_2}^W))\}$ . The probability distribution  $\{p_{j_\ell}^V\}$  has a spread quantified by the Shannon entropy  $H_{\text{Sh}}(\{p_{j_\ell}^V\}) := -\sum_{j_\ell} p_{j_\ell}^V \log p_{j_\ell}^V$ . The left-hand side of Ineq. (24) reduces to  $2[H_{\text{vN}}(W(t))_\rho + H_{\text{Sh}}(\{p_{j_\ell}^V\})]$ .

## II I. Numerical simulations of a spin chain

We illustrate Theorem 1 with an interacting spin chain. The setup and weak-measurement implementation are described in Sec. II I 1. The detector probabilities  $p_{j_\ell}^V$ , the weak-measurement Kraus operators  $K_{j_\ell}^{V, v_\ell}$ , the couplings  $g_{j_\ell}^V$ , and the entropies  $H_\alpha$  are presented in Sec. II I 2 and calculated in App. B. We present and analyze results in Sec. II I 3.

### II I 1. Spin-chain setup

Consider a one-dimensional (1D) chain of  $N = 8$  qubits. The OTOC operators manifest as single-qubit Pauli operators:  $V = \sigma_1^z$ , and  $W = \sigma_N^z$ . The operators' precise forms do not impact our chaotic-system results, however.

**Model:** The chain evolves under the power-law quantum Ising Hamiltonian

$$H_{\text{PQIM}} = -J \sum_{\ell=1}^{\ell_0} \sum_{j=1}^{N-\ell} \frac{1}{\ell^\zeta} \sigma_j^z \sigma_{j+\ell}^z - h^x \sum_{j=1}^N \sigma_j^x - \sum_{j=1}^N h_j^z \sigma_j^z \quad (31)$$

[72] (see [73] for a similar model). Each spin  $j$  interacts with each spin that lies within a distance  $\ell_0$ . The interaction strength declines with distance as a power law controlled by  $\zeta > 0$ . We choose  $J = 1$ ,  $\zeta = 6$ , and  $\ell_0 = 5$ , as in [72]. Planck's constant is set to one:  $\hbar = 1$ . We set the transverse field  $h^x$  to 1.05. The longitudinal field  $h_j^z = 0.375(-1)^j$  flips from site to site.

The transverse-field Ising model with a longitudinal field reproduces our results' qualitative features. But the power-law quantum Ising model mimics all-to-all interactions, such as in the SYK model [19, 28, 54, 55]. Around

<sup>6</sup> This expectation is borne out when  $v_1 = v_2$ , as implied by (i) App. C and (ii) reasoning, similar to that in the appendix, about the  $|g_j^V|^2$  terms in Eq. (26). Appendix C also shows why the quasiprobability tightens the bound when (i)  $v_1 = -v_2$  and (ii)  $g_{j_1}^V g_{j_2}^V$  approximately equals a negative real number.

$t = t_*$ , therefore, the OTOC decays almost exponentially. Exponential decay evokes classical chaos, as discussed in the introduction.

**Weak-measurement implementation:** Section II H guides our implementation, which parallels [44]. We illustrate with the forward-protocol weak measurement, temporarily reinstating operators' hats.

The detector consists of a particle that scatters off the system. The detector could manifest as a photon, as in circuit QED [74] and in purely photonic experiments [75]. Let  $\hat{\mathbf{y}}$  denote the longitudinal direction, which points from the detector's initial position to the system.

Let  $\hat{\mathbf{x}}$  denote a transversal direction; and  $|D\rangle$ , the  $\hat{\mathbf{x}}$  component of the detector's initial state.  $|D\rangle$  consists of a Gaussian,

$$|D\rangle = \frac{1}{\pi^{1/4} \sqrt{\Delta}} \int_{-\infty}^{\infty} dp e^{-p^2/2\Delta^2} |p\rangle, \quad (32)$$

centered on the transverse-momentum eigenvalue  $p \equiv p_x = 0$ .  $\Delta$  denotes the Gaussian's standard deviation.

The displaced detector position  $\hat{x} - x_0 \hat{\mathbb{1}}$  couples<sup>7</sup> to the system's  $\hat{\Pi}_{v_\ell}^{\hat{V}}$ . [The displacement prevents the minimization in (26) from choosing the detector-measurement outcome  $x = 0$ . This choice would set  $g_{x_\ell}^V$  to  $g_{x_0}^V = 0$ , eliminating the weak measurement.] The interaction unitary has the form

$$\hat{V}_{\text{int}} = \exp \left( -\frac{i}{\hbar} \tilde{g} [\hat{x} - x_0 \hat{\mathbb{1}}] \otimes \hat{\Pi}_{v_\ell}^{\hat{V}} \right) \quad (33)$$

$$= \hat{\mathbb{1}} + \left( e^{-\frac{i}{\hbar} \tilde{g} (\hat{x} - x_0 \hat{\mathbb{1}})} - \hat{\mathbb{1}} \right) \otimes \hat{\Pi}_{v_\ell}^{\hat{V}}. \quad (34)$$

The interaction strength  $\tilde{g}$  governs the outcome-dependent coupling  $g_{j_\ell}^{\hat{V}}$ . Numerical experiments show that  $\tilde{g} = 0.02$  and  $x_0 = 10$  keep  $\frac{g_{j_\ell}^{\hat{V}}}{\sqrt{p_{x_\ell}^V}}$  perturbatively small while strengthening the bound.

The detector's  $\hat{x}$  is measured strongly. Let  $L > 0$  denote the measurement's precision. Positions  $x_1$  and  $x_2$  can be distinguished if they lie a distance  $|x_2 - x_1| \geq L$  apart. Hence the classical register has a discrete spectrum  $\{x_\ell\}$ . We simulated a register whose  $L = 0.1$ .

## II I 2. Analytical ingredients in spin-chain uncertainty relation

Analytical results are presented here: the detector probability  $p_{j_\ell}^{\hat{V}} \equiv p_{x_\ell}^{\hat{V}}$ , the weak-measurement Kraus operators  $\hat{K}_{j_\ell}^{\hat{V},v_\ell} \equiv \hat{K}_{x_\ell}^{\hat{V},v_\ell}$ , the coupling strengths  $g_{j_\ell}^{\hat{V}} \equiv g_{x_\ell}^{\hat{V}}$ , and the entropies  $H_\alpha$ . We derive these results and check their practicality in App. B. We remove operators' hats.

Consider preparing the detector in  $|D\rangle$ , then measuring  $\hat{x}$ . The measurement has a probability  $p_{x_\ell}^{\hat{V}} L = |\langle x_\ell | D \rangle|^2 L$  of yielding a position within  $L$  of  $x_\ell$ . By Eq. (32),

$$p_{x_\ell}^{\hat{V}} L = \frac{L \Delta}{\sqrt{\pi} \hbar} e^{-\Delta^2 (x_\ell)^2 / \hbar^2}. \quad (35)$$

The weak-measurement Kraus operators have the form

$$\hat{K}_{x_\ell}^{\hat{V},v_\ell} = \sqrt{p_{x_\ell}^{\hat{V}}} \hat{\mathbb{1}} + g_{x_\ell}^{\hat{V}} \hat{\Pi}_{v_\ell}^{\hat{V}}. \quad (36)$$

The outcome-dependent coupling is

$$g_{x_\ell}^{\hat{V}} = \sqrt{p_{x_\ell}^{\hat{V}}} \left( e^{-\frac{i}{\hbar} \tilde{g} (x_\ell - x_0)} - 1 \right). \quad (37)$$

The Rényi- $\alpha$  entropy limits, as  $\alpha \rightarrow \infty$ , to

$$\begin{aligned} H_{\min}(VW(t))_\rho &= H_{\min} \left( \left\{ p_{j_1}^V \right. \right. \\ &\quad \left. \left. + 2\sqrt{p_{j_1}^V} \text{Re} \left( g_{j_1}^V \text{Tr} \left( \Pi_{w_1}^{W(t)} \Pi_{v_1}^V \rho \right) \right) \right. \right. \\ &\quad \left. \left. + |g_{j_1}^V|^2 \text{Tr} \left( \Pi_{v_1}^V \Pi_{w_1}^{W(t)} \Pi_{v_1}^V \rho \right) \right\}_{v_1,j_1,w_1} \right). \end{aligned} \quad (38)$$

The other entropies have analogous forms.

**Entropies  $H_\alpha$ :** Let us remove operators' hats. We illustrate the entropies' analytical forms with

$$H_{\min}(VW(t))_\rho \equiv H_{\min}(\rho_F) \quad (39)$$

$$= H_{\min} \left( \left\{ \text{Tr} \left( \sqrt{M_{j_1,w_1}^{F,v_1}}^\dagger \sqrt{M_{j_1,w_1}^{F,v_1}} \rho \right) \right\}_{v_1,j_1,w_1} \right). \quad (40)$$

The measurement operators have the form

$$\sqrt{M_{j_1,w_1}^{F,v_1}}^\dagger \sqrt{M_{j_1,w_1}^{F,v_1}} = \left( K_{j_1}^{V,v_1} \right)^\dagger \Pi_{w_1}^{W(t)} K_{j_1}^{V,v_1}, \quad (41)$$

by Eq. (13). We substitute in from Eq. (12), multiply out, and substitute into Eq. (40):

$$\begin{aligned} H_{\min}(VW(t))_\rho &= H_{\min} \left( \left\{ p_{j_1}^V \right. \right. \\ &\quad \left. \left. + 2\sqrt{p_{j_1}^V} \text{Re} \left( g_{j_1}^V \text{Tr} \left( \Pi_{w_1}^{W(t)} \Pi_{v_1}^V \rho \right) \right) \right. \right. \\ &\quad \left. \left. + |g_{j_1}^V|^2 \text{Tr} \left( \Pi_{v_1}^V \Pi_{w_1}^{W(t)} \Pi_{v_1}^V \rho \right) \right\}_{v_1,j_1,w_1} \right). \end{aligned} \quad (42)$$

The other entropies have analogous forms.

<sup>7</sup>  $\hat{\Pi}_{v_\ell}^{\hat{V}}$  can effectively be measured weakly via coupling of the detector to  $V = \hat{\sigma}_\ell^z$ . The interaction unitary will have the form  $\exp(-\frac{i}{\hbar} \tilde{g} [\hat{x} \otimes \hat{\sigma}_\ell^z])$ . The Pauli operator decomposes as  $\hat{\sigma}_\ell^z = \pm (2\hat{\Pi}_\pm^{\hat{V}} - \hat{\mathbb{1}})$ . Hence the interaction unitary has the form  $\exp(\pm \frac{i}{\hbar} \tilde{g} [\hat{x} \otimes \hat{\mathbb{1}}]) \exp(\mp \frac{2i}{\hbar} \tilde{g} [\hat{x} \otimes \hat{\Pi}_\pm^{\hat{V}}])$ . The Kraus operator becomes  $\langle x_\ell | \exp(\pm \frac{i}{\hbar} \tilde{g} [\hat{x} \otimes \hat{\mathbb{1}}]) \exp(\mp \frac{2i}{\hbar} \tilde{g} [\hat{x} \otimes \hat{\Pi}_\pm^{\hat{V}}]) |D\rangle$ . The lefthand exponential can be absorbed into the strong measurement of the detector: Consider wishing to measure  $\hat{\Pi}_+^{\hat{V}}$  weakly. Instead of measuring the detector's  $\{|x_\ell\rangle\}$  strongly, one measures  $\{e^{-\frac{i}{\hbar} \tilde{g} \hat{x}} |x_\ell\rangle\}$ .

### II I 3. Spin-chain results

Figures 1-3 illustrate the entropic uncertainty relations for information scrambling [Ineqs. (24) and (25)] in the characteristic parameter regime detailed in Sec. II I 2. Time is measured in units of the inverse coupling,  $1/J = 1$ . The scrambling time  $t_* \approx 4$ , as reflected by (i) the quasiprobability's sharp change in Fig. 2 and (ii) the OTOC's decay in omitted plots.

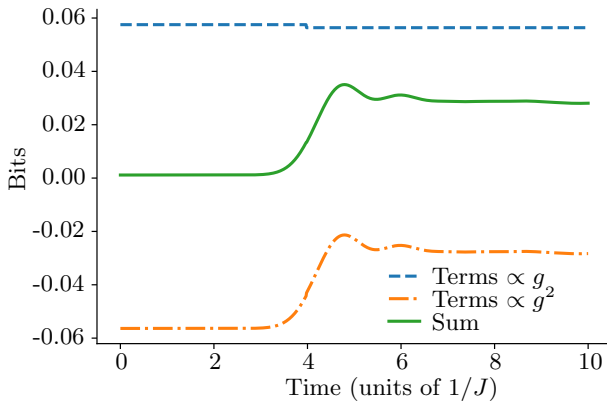
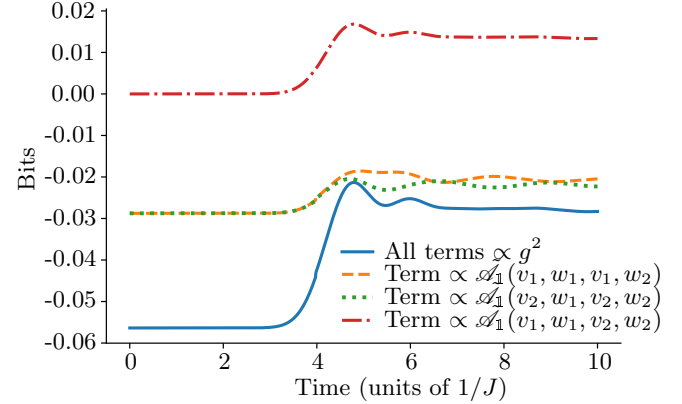


**FIG. 1: Greatest coupling-dependent contributions to the entropic uncertainty bound for scrambling:**

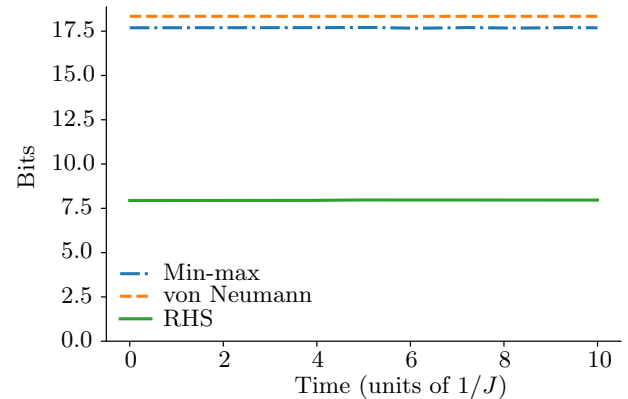
We numerically simulated a one-dimensional chain of  $N = 8$  qubits evolving under the power-law quantum Ising Hamiltonian (31). The nearest-neighbor coupling  $J = 1$ , the transverse field  $h^x = 1.05$ , and  $\zeta = 6$  and  $\ell_0 = 5$  govern the interactions' power-law decay. The system was initialized in the Gibbs state  $\rho = e^{-\beta H}/Z$  at inverse temperature  $\beta = 1$ . The weak-coupling strength  $\tilde{g} = 0.02$ . The out-of-time-ordered-correlator (OTOC) operators  $V$  and  $W$  manifest as single-qubit Pauli operators localized on opposite sides of the chain:  $V = \sigma_1^z$ , and  $W = \sigma_N^z$ . The greatest coupling-dependent contributions to the entropic uncertainty bound  $f(v_1=1, v_2=-1)$  [Eq. (26)] are plotted against time, measured in units of  $1/J$ . The bound tightens at the scrambling time  $t \approx t_*$ . This growth confirms that Theorem 1 unifies two notions of operator disagreement, entropic uncertainty relations and information scrambling.

Figure 1 shows the greatest time-dependent contributions to the bound  $f(v_1, v_2)$  [Eq. (26)]. Choosing  $v_1 = -v_2$  tightens the bound (see App. C), so we focused on  $v_1 = 1$  and  $v_2 = -1$ . The bound grows at  $t = t_*$ , confirming expectations: At the scrambling time, the OTOC drops. A decayed OTOC reflects noncommutation of  $V$  and  $W(t)$ . The worse two operators commute, the stronger their entropic uncertainty relations; the stronger the uncertainty bound  $f(v_1, v_2)$ . Hence Theorem 1 unites information scrambling and OTOCs with entropic uncertainty relations, as claimed.

Figure 2 shows the quasiprobability's contribution to the uncertainty bound (26). Figure 3 shows the LHS of Ineq. (24) ( $H_{vN} + H_{vN}$ ), the LHS of Ineq. (25) at  $(\alpha, \beta) = (\infty, 1/2)$  ( $H_{\min} + H_{\max}$ ), and the shared RHS



**FIG. 2: Quasiprobability's contribution to the entropic uncertainty bound for scrambling:** The quasiprobability  $\tilde{A}_1$  governs three terms in the bound  $f(v_1=1, v_2=-1)$  [Eq. (26)]; these terms are plotted against time. The system parameters are those described below Fig. 1.



**FIG. 3: Left-hand and right-hand sides of two entropic uncertainty relations for information scrambling:** The orange, dashed curve illustrates the  $H_{vN} + H_{vN}$  of Ineq. (24). The blue, dash-dotted curve illustrates the  $H_{\min} + H_{\max}$  of Ineq. (25) for  $(\alpha, \beta) = (\infty, 1/2)$ . The green, solid curve of Eq. (26) illustrates the bound  $f(v_1=1, v_2=-1)$ . The system parameters are those described below Fig. 1. The bound's tightening is undetectable due to the  $y$ -axis scale.

$f(v_1, v_2)$ . Figure 3 is more zoomed-out than Fig. 2; hence the tightening is too small to detect. This reduced visibility is expected: Scrambling is a subtle, high-order stage of quantum equilibration. It manifests in the  $g^2$  terms of  $f(v_1, v_2)$ , just as  $\tilde{A}_\rho$  can be inferred from high-order terms in weak-measurement experiments [35, 36].

The LHSs lie  $\sim 10$  bits above the bound. The gap stems from the  $\text{Tr}(\Pi_{w_2}^W) = 2^{N-1}$  in Eq. (26). This gap bodes ill for the large-system limit,  $N \rightarrow \infty$ , of interest in holography. But the gap scales only linearly, not exponentially, with  $N$ . Furthermore, small gaps would

follow from many of today's experiments (e.g., [76]). Additionally, Sec. II K presents weak-measurement entropic uncertainty relations independent of scrambling. Those uncertainty relations need not have such a gap. We will illustrate with a qubit example whose bound is tight at zeroth order in  $g$ , in Sec. II K.

Figure 4 illustrates how tight the bound can grow in an exceptional parameter regime. The top curves represent  $H_{\min} + H_{\max}$  and  $H_{\text{vN}} + H_{\text{vN}}$ . These curves dip at  $t \approx t_*$  because (i)  $\rho$  is a  $W(t \approx t_*)$  eigenstate and (ii) the POVMs'  $W(t)$  measurements are fine-grained—are replaced with measurements of  $\{U^\dagger|w_\ell, \alpha_{w_\ell}\rangle U\}$ . The POVM outcomes become highly predictable around  $t_*$ , so the bound grows tight to within 0.53 bits.<sup>8</sup>

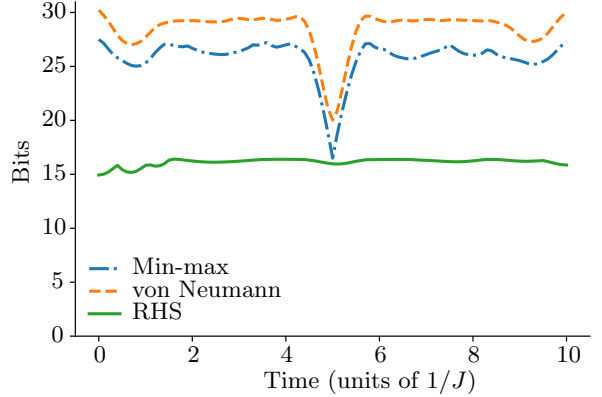


**FIG. 4: Strengthened bound in exceptional parameter regime:** The system parameters have the values below Fig. 1, with three exceptions. First, the initial state  $\rho$  is a  $W(t)$  eigenstate, wherein the time  $t$  is evaluated at the scrambling time  $t_*$ . Second, the  $W(t)$  measurements in the positive operator-valued measures (13) and (14) are fine-grained [are measurements of a  $W(t)$  eigenbasis, rather than measurements of  $W(t)$ ]. The orange, dashed curve illustrates  $H_{\text{vN}} + H_{\text{vN}}$  [Ineq. (24)]. The blue, dash-dotted curve illustrates  $H_{\min} + H_{\max}$  [Ineq. (25) at  $(\alpha, \beta) = (\infty, 1/2)$ ]. The upper curves drop to within 0.53 bits of the bound (the green, solid curve). Third, the Hamiltonian interaction strength  $\tilde{g} = 0.16$ , rendering the measurement-dependent coupling strengths  $g_{x_1, x_2}^V$  comparable to the detector probabilities  $p_{x_1, x_2}^V$ . This comparability invalidates the Taylor expansion that leads to Eq. (26). The bound given by (26) appears as the green, solid curve.

Our numerics emphasize the scrambling Hamiltonian  $H_{\text{PQIM}}$ , which is nonintegrable. Integrable Hamiltonians' OTOCs revive and decay repeatedly, as information recollects from across the system and spreads again. The revivals and decays lift and suppress  $f(v_1, v_2)$ , we have confirmed using a transverse-field Ising model. The relevant plots are omitted but appear at [77].

## II J. Extension to higher-point OTOCs

Higher-point OTOCs reflect later, subtler stages of QI scrambling and many-body equilibration.  $F(t)$  has been generalized to the  $\mathcal{K}$ -fold OTOC [36, 38–42]

$$F^{(\mathcal{K})}(t) := \langle A(t_1)B(t_2)C(t_3) \dots, E(t_{\mathcal{K}})F(t_{\mathcal{K}+1})G(t_{\mathcal{K}+2}) \dots Q(t_{2\mathcal{K}-1})R(t_{2\mathcal{K}}) \rangle. \quad (43)$$

We follow the notation in [36]. This  $2\mathcal{K}$ -point correlator is labeled by  $\mathcal{K} = 1, 2, 3, \dots$ . The conventional OTOC corresponds to  $\mathcal{K} = 2$ . If  $F^{(\mathcal{K})}(t) = \langle W(t)V \dots W(t)V \rangle$ , the correlator encodes  $\mathcal{K}$  time reversals, as concretized in Schwinger-Keldysh path integrals [39] and in the weak-measurement scheme [35, 36]. Higher-point OTOCs  $F^{(\mathcal{K})}(t)$  equilibrate at later times

<sup>8</sup> In addition to choosing  $\rho$  and to fine-graining, we raised the interaction strength to  $\tilde{g} = 0.16$ . The outcome-dependent coupling strengths  $g_{x_\ell}^V$  are comparable to the detector probabilities:  $g_{x_\ell}^V \approx p_{x_\ell}^V$ . This comparability invalidates the Taylor expansion that leads to Eq. (26). Equation (A15) in App. A gives the pre-Taylor-expansion bound. This bound appears as the solid, green, bottom curve in Fig. 4. The bound would rise more than in the earlier figures, if the POVMs'  $W(t)$  measurements remained fine-grained: The large  $g$ 's would magnify the  $\mathcal{A}_1$  term's rise. Since the  $W(t)$  measurements are fine-grained, the POVMs cease to capture the spirit of scrambling, defined in terms of local  $V$  and  $W$ . Hence we should not necessarily expect scrambling to lift the bound.

$t_*^{(\mathcal{K})} \sim (\bar{\mathcal{K}} - 1)t_*$  [42] and can be inferred from sequences of  $2\bar{\mathcal{K}} - 1$  weak measurements.

$F^{(\bar{\mathcal{K}})}(t)$  equals a coarse-graining of a quasiprobability distribution  $\tilde{\mathcal{A}}_\rho^{(\bar{\mathcal{K}})}$  [36].  $\tilde{\mathcal{A}}_\rho^{(\bar{\mathcal{K}})}$  governs terms  $\propto g^{2(\bar{\mathcal{K}}-1)}$  in an entropic uncertainty relation for scrambling. Denote the eigenvalues of  $A(t_1), B(t_2), \dots$  by  $a, b, \dots$  Denote the eigensubspace projectors by  $\Pi_a^{A(t_1)}, \Pi_b^{B(t_2)}, \dots$  The forward POVM consists of a weak measurement of  $\Pi_r^{R(t_{2\bar{\mathcal{K}}})}$ , followed by a weak measurement of  $\Pi_q^{Q(t_{2\bar{\mathcal{K}}-1})}$ , and so on, until a weak measurement of  $\Pi_g^{G(t_{\bar{\mathcal{K}}+2})}$ , followed by a strong measurement of  $F(t_{\bar{\mathcal{K}}+1})$ . The reverse POVM consists of a strong measurement of  $A(t_1)$ , followed by a weak measurement of  $\Pi_b^{B(t_2)}$ , followed by more weak measurements, until a weak measurement of  $\Pi_e^{E(t_{\bar{\mathcal{K}}})}$ .

The weak measurement of an observable  $\Theta = B(t_2), C(t_3), \dots$  is represented by a Kraus operator  $K_{j_\alpha}^{\Theta, \theta_\alpha} = p_{j_\alpha}^\Theta \mathbb{1} + g_{j_\alpha}^\Theta \Pi_\alpha^\Theta$ . The  $j_\alpha$  denotes the weak measurement's outcome,  $p_{j_\alpha}^\Theta$  denotes the detector probability, and  $g_{j_\alpha}^\Theta$  denotes the outcome-dependent weak-coupling strength.

The von Neumann uncertainty relation has the form

$$\begin{aligned} & H(A(t_1)B(t_2) \dots E(t_{\bar{\mathcal{K}}})) \\ & + H(R(t_{2\bar{\mathcal{K}}})Q(t_{2\bar{\mathcal{K}}-1}) \dots F(t_{\bar{\mathcal{K}}+1})) \\ & \geq -\log \left( p_{j_b}^{B(t_2)} p_{j_c}^{C(t_3)} \dots p_{j_e}^{E(t_{\bar{\mathcal{K}}})} p_{j_g}^{G(t_{\bar{\mathcal{K}}+2})} \dots p_{j_q}^{Q(t_{2\bar{\mathcal{K}}-1})} \right. \\ & \quad \times \text{Tr} \left( \Pi_a^{A(t_1)} \Pi_f^{F(t_{\bar{\mathcal{K}}+1})} \right) \left. \right) \\ & + (\text{g-dependent terms}). \end{aligned} \quad (44)$$

The term

$$\left( g_{j_b}^{B(t_2)} g_{j_c}^{C(t_3)} \dots g_{j_e}^{E(t_{\bar{\mathcal{K}}})} \right) \left( g_{j_g}^{G(t_{\bar{\mathcal{K}}+2})} \dots g_{j_q}^{Q(t_{2\bar{\mathcal{K}}-1})} \right) \times \tilde{\mathcal{A}}_\rho^{(\bar{\mathcal{K}})}(r, q, \dots, a) \quad (45)$$

contains the quasiprobability behind the  $\bar{\mathcal{K}}$ -fold OTOC.<sup>9</sup> Hence our entropic uncertainty relations extend to arbitrary-point OTOCs.

<sup>9</sup> Entropic uncertainty relations for  $\geq 3$  measurements have been derived [16]. Could such relations contain  $\bar{\mathcal{K}}$ -fold OTOCs? The match appears unnatural, for two reasons. First, consider the minimal generalization of  $F(t)$ , in which every observable equals  $W(t)$  or  $V$ :  $\langle W(t)V \dots W(t)V \rangle$ . Each POVM involves only two observables,  $W(t)$  and  $V$ , not three observables.

Second, suppose that (i)  $A, \dots, R$  are unitary, as well as Hermitian, and (ii)  $\rho$  is pure.  $|F^{(\bar{\mathcal{K}})}|$  equals an overlap  $|\langle \psi'_{\text{II}} | \psi'_{\text{I}} \rangle|$ , as  $F(t)$  was shown to in the introduction. Implementing  $A(t_1)$ , then  $B(t_2)$ , etc., then  $E(t_{\bar{\mathcal{K}}})$  prepares  $|\psi'_{\text{II}}\rangle$ . Implementing an analogous sequence prepares  $|\psi'_{\text{II}}\rangle$ . The overlap  $|F^{(\bar{\mathcal{K}})}|$  compares one sequence to the other, rather than comparing all the observables that define the sequences. An entropic uncertainty relation, in contrast, reflects all the observables' disagreements with each other.

## II K. Entropic uncertainty relations for weak values beyond scrambling

Weak values, like OTOCs, involve time reversals and measurement sequences [44, 45]. Consider preparing a quantum system in a state  $|i\rangle$  at a time  $t = 0$ , evolving the system for a time  $t''$  under a unitary  $U_{t''}$ , measuring a nondegenerate observable  $F = \sum_f f |f\rangle\langle f|$ , and obtaining the outcome  $f$ . Let  $A = \sum_a a |a\rangle\langle a|$  denote a nondegenerate observable that fails to commute with  $F$ .

Which value can most reasonably be attributed, retrodictively, to the  $A$  at a time  $t' \in (0, t'')$ , given that  $|i\rangle$  was prepared and that the measurement yielded  $f$ ? The *weak value*

$$A_{\text{wk}} := \frac{\langle f' | A | i' \rangle}{\langle f' | i' \rangle}, \quad (47)$$

is the expectation value conditioned on the preselection and postselection.  $|f'\rangle := U_{t''-t'}|f\rangle$  and  $|i'\rangle := U_{t'}|i\rangle$  denote time-evolved states.

Consider eigendecomposing  $A$ , then factoring out the sum and eigenvalues. Multiplying the numerator and denominator by  $\langle i' | f' \rangle$  yields

$$A_{\text{wk}}(i, f) = \sum_a a \frac{\langle f' | a \rangle \langle a | i' \rangle \langle i' | f' \rangle}{p(f|i)}, \quad (48)$$

wherein  $p(f|i) = |\langle f' | i' \rangle|^2$  denotes a conditioned probability. The numerator is a *Kirkwood-Dirac quasiprobability* [78, 79], an extension of which is the OTOC quasiprobability [36]. The Kirkwood-Dirac quasiprobability governs the conditional quasiprobability  $\langle f' | a \rangle \langle a | i' \rangle \langle i' | f' \rangle / p(f|i)$  that, if  $|i\rangle$  is prepared and the  $F$  measurement yields  $f$ ,  $a$  is the value most reasonably attributable to  $A$  retrodictively.

$A_{\text{wk}}$  generalizes to arbitrary initial states  $\rho$  and to degenerate observables  $A = \sum_a a \Pi_a^A$  and  $F = \sum_f f \Pi_f^F$ :

$$A_{\text{wk}}(\rho, f) = \frac{\text{Tr} \left( \Pi_f^{F(t''-t')} A \rho(t') \right)}{p(f|\rho)}. \quad (49)$$

The time-evolved state  $\rho(t') := U_{t'}^\dagger \rho U_{t'}$ , and the conditional probability  $p(f|\rho) := \text{Tr} \left( \Pi_f^{F(t''-t')} \rho(t') \right)$ . One can infer  $A_{\text{wk}}$  experimentally by preparing  $\rho$ , evolving the system for a time  $t'$ , measuring  $A$  weakly, evolving the system for a time  $t'' - t'$ , and measuring  $F$  strongly. One performs this protocol in many trials.  $A_{\text{wk}}$  is inferred from the measurement statistics.

$A_{\text{wk}}$  can range outside the spectrum of  $A$ , as advertised in the foundational paper [44]. Hence the physical significances of  $A_{\text{wk}}$  have galvanized debate (e.g., [80–87]). Weak values have been interpreted in terms of conditioned expectation values [44] and disturbances by measurements [88]. Kirkwood-Dirac quasiprobabilities have been interpreted in terms of operator decompositions [75, 89] and Bayesian retrodiction [44, 87, 90–92].

We introduce another physical significance: Weak values govern first-order-in- $g$  terms in entropic uncertainty bounds for POVMs that involve weak measurements. Kirkwood-Dirac quasiprobabilities play an analogous role in analogous bounds. We present the results in Sec. II K 1, then illustrate with a qubit in Sec. II K 2.

### II K 1. Entropic uncertainty relations for weak values and Kirkwood-Dirac quasiprobabilities

Consider a quantum system associated with a Hilbert space  $\mathcal{H}$ . Let  $\rho \in \mathcal{D}(\mathcal{H})$  denote any state of the system. Let  $A = \sum_a a \Pi_a^A$ ,  $F = \sum_f f \Pi_f^F$ , and  $\mathcal{I} = \sum_i \lambda_i \Pi_i^I$  be eigenvalue decompositions of observables. [The index  $i$  should not be confused with  $\sqrt{-1}$ . The index serves similarly to the  $i$  that labels the initial state  $|i'\rangle$  in Eq. (50).]

The uncertainty relation for  $A_{\text{wk}}$  features a POVM that we label I. One measures  $A$  weakly, then  $F$  strongly:  $\{\sqrt{M_{j,f}^I} := \Pi_f^F K_j^A\}$ . The weak-measurement Kraus operator  $K_j^A = \sqrt{p_j^A} \mathbb{1} + g_j^A A + O(g^2)$ . The  $O(g^2)$  signifies terms of second order in the Hamiltonian's coupling parameter (e.g., the  $\tilde{g}$  in the spin-chain example of Sec. II I). We define as POVM II a strong measurement of  $\mathcal{I}$ :  $\{\sqrt{M_i^{\text{II}}} := \Pi_i^{\mathcal{I}}\}$ .

Define the entropies  $H_\alpha(AF)_\rho$ , and  $H_\alpha(\mathcal{I})_\rho$  via analogy with the QI-scrambling entropies (Sec. II F). One can infer the weak value<sup>10</sup>

$$A_{\text{wk}}(i, f) = \frac{\text{Tr}(\Pi_f^F A \Pi_i^{\mathcal{I}})}{\text{Tr}(\Pi_f^F \Pi_i^{\mathcal{I}}) \text{Tr}(\Pi_i^{\mathcal{I}})} \quad (50)$$

by preparing the state  $\Pi_i^{\mathcal{I}}/\text{Tr}(\Pi_i^{\mathcal{I}})$ , measuring  $A$  weakly, and postselecting a strong  $F$  measurement on  $f$ .

**Theorem 2.** *POVMs I and II obey entropic uncertainty relations dependent on the weak value  $A_{\text{wk}}(i, f)$ :*

$$H_{\text{vN}}(\mathcal{I})_\rho + H_{\text{vN}}(AF)_\rho \geq f_{\text{wk}}, \quad \text{and} \quad (51)$$

$$H_\alpha(\mathcal{I})_\rho + H_\beta(AF)_\rho \geq f_{\text{wk}}. \quad (52)$$

The bound has the form

$$f_{\text{wk}} := \min_{i,j,f} \left\{ -\log(p_j^A \text{Tr}(\Pi_f^F \Pi_i^{\mathcal{I}})) - \frac{2}{\ln 2} \frac{\text{Tr}(\Pi_i^{\mathcal{I}})}{\sqrt{p_j^A}} \text{Re}(g_j^A A_{\text{wk}}(i, f)) + O(g^2) \right\}. \quad (53)$$

The Rényi orders  $\alpha$  and  $\beta$  satisfy  $\frac{1}{\alpha} + \frac{1}{\beta} = 2$ , and  $\rho$  denotes an arbitrary state.

<sup>10</sup> We have tweaked our notation for  $A_{\text{wk}}$ . The first argument  $i$ , labels the subspace over which the state  $\Pi_i^{\mathcal{I}}/\text{Tr}(\Pi_i^{\mathcal{I}})$  is maximally mixed.

The proof is analogous to the proof of Theorem 1. The forward and reverse POVMs are replaced with POVMs I and II. One can prove analogous uncertainty relations in which Kirkwood-Dirac quasiprobabilities replace  $A_{\text{wk}}$ . The weak measurement of  $A$  gives way to a weak measurement of an  $A$  eigenprojector. The uncertainty bound (52) can be smoothed when  $(\alpha, \beta) = (\infty, 1/2)$ . For uncertainty relations that involve weak measurements, but are not entropic, see [93].

### II K 2. Qubit example

Let us illustrate the uncertainty relation (52) for  $(\alpha, \beta) = (\infty, 1/2)$ . The system, denoted by a subscript  $s$ , consists of a qubit. So does the detector, denoted by  $d$ . Let  $\mathcal{I} = \sigma_s^z$ ,  $A = \sigma_s^y$ , and  $F = \sigma_s^x$ .

The weak measurement manifests as follows: The detector begins in the state  $|z+\rangle$ , a  $z$ -controlled  $y$  couples the system to the detector weakly, and the detector's  $\sigma_d^y$  is measured strongly. The weak values  $A_{\text{wk}}(z_s, x_s) = x_s z_s i$  are imaginary and so nonclassical [88]:  $A$  has only real eigenvalues  $a$ , but the conditioned average  $A_{\text{wk}}$  is imaginary.

We illustrate the uncertainty relation's LHS with  $\rho = |z+\rangle\langle z+|$ . The inequality is calculated in App. D:  $2.00 \geq 2.00 - \frac{2}{\ln 2} |\tilde{g}| + O(\tilde{g}^2)$ . If  $\tilde{g} = 2.00 \times 10^{-2}$ , as in Sec. II I, the relation approximates to  $2.00 \geq 1.94$ . The bound is satisfied and is tight at order  $g^0$ .

## III. DISCUSSION

We have reconciled two measures of disagreement between quantum operators: entropic uncertainty relations and out-of-time-ordered correlators (OTOCs). The reconciliation unites several subfields of physics: (i) quasiprobabilities and weak measurements tie (ii) quantum information theory to (iii) condensed matter and (iv) high-energy physics. Information theory and complexity theory have begun intersecting with condensed matter and high-energy physics recently, shedding light on black holes, information propagation, and space-time (e.g., [26, 94–99]). This paper broadens the intersection into quasiprobability and quantum-measurement theory and farther into quantum information theory.

This broadening has two more important significances: one for OTOC theory and one for weak-measurement theory. First, the extension reconciles the OTOC's  $V$  with the tiny perturbation that triggers violent consequences in the classical butterfly effect:  $V$  can naturally be regarded, our uncertainty relations show, as being measured weakly. The weak measurement is perturbative literally, in the coupling strength  $g$ .

Within measurement theory, second, we have uncovered a physical significance of weak values  $A_{\text{wk}}$  and Kirkwood-Dirac quasiprobabilities: These quantities govern first-order terms in entropic uncertainty rela-

tions obeyed by weak measurements. Quantum information theory therefore sheds light on mathematical objects whose interpretations have been debated in quantum optics, quantum foundations, and quantum computation.

In a recent paper, an uncertainty relation was extended to unitaries, then applied to bound the OTOC [100]. OTOC bounds have been known to limit the speed at which many-body entanglement can develop [18, 24, 101]. The present work takes a fundamentally different approach: Scrambling takes central stage in this paper, whose main purpose is to unite two communities' notions of quantum operator disagreement. Additionally, our uncertainty relations are entropic, tapping into recent developments in pure quantum information theory. Finally, our formalism covers both unitary and Hermitian OTOC operators  $V$  and  $W$ .

This work uncovers several research opportunities. Inspired by condensed matter, we have focused on discrete systems. Also continuous systems—quantum field theories (QFTs)—have OTOCs used to study, e.g., black holes in the anti-de-Sitter-space/conformal-field-theory (AdS/CFT) duality [19–25, 30]. Entropic uncertainty relations for continuous-variable systems have been derived [2–4, 102–106]. They should be applied to characterize scrambling in QFTs.

Second, Theorems 1 and 2 can be tested experimentally. The techniques needed exist: OTOC measurements have been proposed in detail [27, 35, 36, 71, 107–111], and early-stage OTOC-measurement experiments have performed [53, 76, 112, 113]; weak values and Kirkwood-Dirac distributions have been measured weakly [75, 89, 114–123]; and entropic uncertainty relations have been tested experimentally [124–127]. Testing Theorem 1 should be feasible in the immediate future, especially through the weak-measurement proposal for inferring the OTOC quasiprobability  $\tilde{\mathcal{A}}_\rho$  [35, 36]. Prospective platforms include superconducting qubits, ultracold atoms, trapped ions, quantum dots, and potentially NMR.

Testing Theorem 2 experimentally requires even fewer resources: Interacting many-body systems are unnecessary, and one weak measurement per trial suffices. Tantalizingly, though, two [128–130] and three [123] sequential weak measurements have been realized recently. They can be applied to (i) characterize higher-order terms in Eqs. (52) and (53), (ii) test entropic uncertainty relations for higher-point OTOCs (Sec. II J), and (iii) test entropic uncertainty relations for POVMs of sequential weak measurements.

Third, the entropic uncertainty relations for scrambling can be smoothed with an error tolerance  $\varepsilon$ . When smoothing, one ignores highly unlikely events [64]. Highly unlikely outcomes of weak-measurement experiments correspond to anomalous weak values and nonclassical quasiprobability values [87]. Nonclassical operator disagreement underlies nontrivial uncertainty relations. Whether smoothing trivializes entropic uncertainty relations for weak measurements merits study. Rough numerical studies suggest that  $\varepsilon$  might actually tighten the

spin-chain bound (25).

Like smoothing, conditioning generalizes the entropic uncertainty relations in [14]. Consider holding a memory  $\sigma$  that is entangled with a to-be-measured state  $\rho$ . Conditioning on  $\sigma$  can change your uncertainty about the measurement outcome. Certain scrambling setups might be cast in terms of a memory  $\sigma$ . An example consists of a qubit chain and an ancilla qubit [131]. Consider entangling the ancilla with the chain's central qubit, then evolving the chain under a many-body Hamiltonian. The entanglement with the ancilla spreads through the chain. The ancilla might be cast as the memory  $\sigma$  in conditioned entropic uncertainty relations for scrambling.

Finally, nonclassicality of  $\tilde{\mathcal{A}}_1$  and  $A_{\text{wk}}$  might strengthen the uncertainty bounds. The quasiprobability behaves nonclassically by acquiring negative real and nonzero imaginary components. The weak value  $A_{\text{wk}}$  behaves nonclassically by lying outside the spectrum of  $A$ . Such nonclassical mathematical behavior can signal nonclassical physics [57–60, 132, 133]. The quasiprobability's nonclassicality features little in our numerical example (Sec. II I): First, the quasiprobability's imaginary part vanishes when evaluated on  $\mathbb{1}$  [36, Sec. III and Sec. V A]. Hence  $\text{Im}(\tilde{\mathcal{A}}_1)$  cannot influence the bound. Second,  $\tilde{\mathcal{A}}_1$  assumes negative values, but not when  $w_1 = w_2$ . Higher-point-OTOC quasiprobabilities could avoid this roadblock, and assume negative values in the bound, as higher-point forward and reverse protocols depend on weak  $W(t)$  measurements (Sec. II J). Nonclassicality's potential to tighten uncertainty bounds merits study.

#### IV. DATA AVAILABILITY

The simulation data and code are available at [77].

**Author contributions:** All authors contributed to this paper equally.

**Competing financial interests:** The authors declare no competing financial interests.

#### ACKNOWLEDGMENTS

We are grateful for conversations with Fernando G. S. L. Brandão, Sean Carroll, Justin Dressel, Patrick Hayden, José Raúl Gonzalez Alonso, Renato Renner, Brian Swingle, and Marco Tomamichel. NYH is grateful for support from the Institute for Quantum Information and Matter (IQIM), for a Barbara Groce Graduate Fellowship, and for a Graduate Fellowship from the Kavli Institute for Theoretical Physics. NYH acknowledges Mark van Raamsdonk, his fellow conference organizers, the “It from Qubit” collaboration, and UBC for their hospitality and their invitation to participate in “Quantum Information in Quantum Gravity III,” where this project partially took shape. AB acknowledges support from

the Walter Burke Institute for Theoretical Physics and the U.S. Department of Energy, Office of Science, Office of High Energy Physics, under Award Number DE-SC0011632. JP is supported partially by the Simons Foundation and partially by the Natural Sciences and

Engineering Research Council of Canada. The IQIM is an NSF Physics Frontiers Center (NSF Grant PHY-1125565) that receives support from the Gordon and Betty Moore Foundation (GBMF-2644). The KITP is supported by the NSF under Grant No. NSF PHY-1125915.

## Appendix A PROOF OF THEOREM 1

Tomamichel presents an entropic uncertainty relation for the smooth entropies  $H_{\min}^\varepsilon$  and  $H_{\max}^\varepsilon$  [14, Result 7]; Krishna and Parthasarathy derive one for  $H_{\text{vN}}$  and  $H_{\text{vN}}$  [61, Corollary 2.6]; and Rastegin presents one for  $H_\alpha$  and  $H_\beta$  [70, Ineq. (13)] (proved in [134]). We use Tomamichel's notation, for concreteness. But the three uncertainty relations have the same RHSs. Hence our use of [14, Result 7] translates directly into uses of the other two bounds.

Tomamichel considers POVMs  $\mathcal{X}$  and  $\mathcal{Y}$  whose outcomes are recorded in classical registers  $X$  and  $Y$ . The systems  $B$  and  $C$  can hold quantum side information about, or have correlations with,  $X$  and  $Y$ . An agent performing an information-processing task might wish to infer about  $X$  and  $Y$ , given access to  $B$  and  $C$ . Tomamichel presents the entropic uncertainty relation

$$H_{\min}^\varepsilon(X|B)_\rho + H_{\max}^\varepsilon(Y|C)_\rho \geq \log \frac{1}{c(\mathcal{X}, \mathcal{Y})} \quad (\text{A1})$$

in [14] (see also [135–137]). The smooth entropies  $H_{\min}^\varepsilon$  and  $H_{\max}^\varepsilon$  follow from extremizing  $H_{\min}$  and  $H_{\max}$ . The POVM overlap  $c$ , defined in Eq. (A3), generalizes the overlap (4).

We set the smoothing parameter  $\varepsilon$  to zero. We also trivialize the conditioning, setting the states of  $B, C \propto \mathbb{1}$ . Let us substitute in the POVMs (13) and (14):

$$H_{\min}(VW(t))_\rho + H_{\max}(W(t)V)_\rho \geq -\log(c \left( \left\{ M_{j_1, w_1}^{\text{F}, v_1} \right\}, \left\{ M_{j_2, v_2}^{\text{R}, w_2} \right\} \right)). \quad (\text{A2})$$

The POVM overlap  $c$  is defined as<sup>11</sup>

$$c \left( \left\{ M_{j_1, w_1}^{\text{F}, v_1} \right\}, \left\{ M_{j_2, v_2}^{\text{R}, w_2} \right\} \right) := \max_{j_1, j_2, w_1, w_2} \left\{ \left\| \sqrt{M_{j_1, w_1}^{\text{F}, v_1}} \sqrt{M_{j_2, v_2}^{\text{R}, w_2}} \right\|^2 \right\}. \quad (\text{A3})$$

The operator norm has the form

$$\left\| \sqrt{M_{j_1, w_1}^{\text{F}, v_1}} \sqrt{M_{j_2, v_2}^{\text{R}, w_2}} \right\| = \lim_{\alpha \rightarrow \infty} \left\{ \text{Tr} \left( \sqrt{\left[ \sqrt{M_{j_1, w_1}^{\text{F}, v_1}} \sqrt{M_{j_2, v_2}^{\text{R}, w_2}} \right]^\dagger \left[ \sqrt{M_{j_1, w_1}^{\text{F}, v_1}} \sqrt{M_{j_2, v_2}^{\text{R}, w_2}} \right]} \right)^\alpha \right\}^{1/\alpha}. \quad (\text{A4})$$

The outer square-root equals, by Eqs. (13) and (14),

$$\sqrt{\sqrt{M_{j_2, v_2}^{\text{R}, w_2}}^\dagger \sqrt{M_{j_1, w_1}^{\text{F}, v_1}}^\dagger \sqrt{M_{j_1, w_1}^{\text{F}, v_1}} \sqrt{M_{j_2, v_2}^{\text{R}, w_2}}} = \sqrt{\Pi_{w_2}^{W(t)} K_{j_2}^{V, v_2} (K_{j_1}^{V, v_1})^\dagger \Pi_{w_1}^{W(t)} K_{j_1}^{V, v_1} (K_{j_2}^{V, v_2})^\dagger \Pi_{w_2}^{W(t)}} \quad (\text{A5})$$

$$\equiv \sqrt{O}. \quad (\text{A6})$$

The two central projectors have collapsed into one:  $\left( \Pi_{w_1}^{W(t)} \right)^2 = \Pi_{w_1}^{W(t)}$ .

<sup>11</sup> Reference [138] strengthens the  $H_{\text{vN}} - H_{\text{vN}}$  bound by replacing  $c(\mathcal{X}, \mathcal{Y})$  with  $c'(\mathcal{X}, \mathcal{Y}) := \min \left\{ \max_x \left\| \sum_y \mathcal{Y}^y \mathcal{X}^x \mathcal{Y}^y \right\|, \max_y \left\| \sum_x \mathcal{X}^x \mathcal{Y}^y \mathcal{X}^x \right\| \right\}$ . (See Sec. III.D of [15] for a review.) That is,  $c$  may be replaced with  $c' \leq c$  in the  $H_{\text{vN}} - H_{\text{vN}}$  version of (A1). (We thank an anonymous reviewer for bringing this result to our attention.) Substituting in our POVMs and Taylor-approximating, as

below, would be straightforward. However, the resulting bound would involve more-complicated operators than our uncertainty bound for scrambling. Identifying OTOC quasiprobabilities in the strengthened bound may therefore be more difficult. Re-engineering the POVMs might enable one to strengthen the bound while retaining the bound's dependence on the OTOC quasiprobability and so the bound's tightening at the scrambling time.

The operator  $O$  is Hermitian and so eigendecomposes. The eigenvalues are real and nonnegative, being the squares of the singular values of  $\sqrt{M_{j_1,w_1}^{F,v_1}}\sqrt{M_{j_2,v_2}^{R,w_2}}$ . Also a physical argument implies the eigenvalues' reality and nonnegativity:  $O$  is proportional to a quantum state:  $\Pi_{w_2}^{W(t)}/\text{Tr}(\Pi_{w_2}^{W(t)})$  represents the state that is maximally mixed over the eigenvalue- $w_2$  eigenspace of  $W(t)$ . Imagine preparing  $\Pi_{w_2}^{W(t)}/\text{Tr}(\Pi_{w_2}^{W(t)})$ , subjecting the state to the quantum channel defined by the operation elements [50]  $\left\{ \left( K_{j_2}^{V,v_2} \right)^\dagger \right\}_{j_2}$ ,<sup>12</sup> subjecting the state to the channel defined by  $\left\{ K_{j_1}^{V,v_1} \right\}_{j_1}$ , and then measuring  $W(t)$  projectively. The resultant state,  $\sigma_f$ , is proportional to  $O$ . The proportionality factor equals  $\text{Tr}(O)$ , the joint probability that (i) this realization of the initial channel's action is labeled by  $j_2$ , (ii) this realization of the second channel's action is labeled by  $j_1$ , and (iii) the  $W(t)$  measurement yields outcome  $w_2$ . Since  $\sigma_f = O/\text{Tr}(O)$   $\sigma_f$  is positive semidefinite and  $\text{Tr}(O)$  equals a probability, the eigenvalues of  $O$  are real and nonnegative.

The eigenvectors of  $O$  are eigenvectors of  $\Pi_{w_2}^{W(t)}$ .  $\Pi_{w_2}^{W(t)}$  has two distinct eigenvalues  $\eta$ :  $\eta = 0$ , of degeneracy  $\text{Tr}(\mathbb{1} - \Pi_{w_2}^{W(t)})$ , and  $\eta = 1$ , of degeneracy  $\text{Tr}(\Pi_{w_2}^{W(t)})$ . Let  $\Lambda_\eta^r$  denote the  $r^{\text{th}}$   $O$  eigenvalue associated with any eigenvector in the  $\eta$  eigenspace of  $\Pi_{w_2}^{W(t)}$ . If  $d_\eta$  denotes the degeneracy of  $\Lambda_\eta^r$ ,  $r = 1, 2, \dots, d_\eta$ . (We have omitted the  $\eta$  dependence from the symbol  $r$  for notational simplicity.) Every eigenvalue-0 eigenvector of  $\Pi_{w_2}^{W(t)}$  is an eigenvalue-0 eigenvector of  $O$ :  $\Lambda_0^r = 0 \ \forall r = 1, 2, \dots, \text{Tr}(\mathbb{1} - \Pi_{w_2}^{W(t)})$ . Hence  $O$  eigendecomposes as

$$O = \sum_{\eta=0}^1 \sum_{r=1}^{d_\eta} \Lambda_\eta^r \Pi_\eta^r = 0 \left( \mathbb{1} - \Pi_{w_2}^{W(t)} \right) + \sum_{r=1}^{d_1} \Lambda_1^r \Pi_1^r. \quad (\text{A7})$$

We use this eigenvalue decomposition to evaluate the RHS of Eq. (A4), working from inside to outside. The outer square-root has the form  $\sqrt{O} = \sum_{r=1}^{d_1} \sqrt{\Lambda_1^r} \Pi_\eta^r$ . The projectors project onto orthogonal subspaces, so  $\left( \sqrt{O} \right)^\alpha = \sum_{r=1}^{d_1} (\Lambda_1^r)^{\alpha/2} \Pi_1^r$ . We take the trace,  $\text{Tr} \left( \left[ \sqrt{O} \right]^\alpha \right) = \sum_{r=1}^{d_1} (\Lambda_1^r)^{\alpha/2}$ , then exponentiate:  $\left\{ \text{Tr} \left( \left[ \sqrt{O} \right]^\alpha \right) \right\}^{1/\alpha} = \left[ \sum_{r=1}^{d_1} (\Lambda_1^r)^{\alpha/2} \right]^{1/\alpha}$ . The limit as  $\alpha \rightarrow \infty$  gives the RHS of Eq. (A4):

$$\left\| \sqrt{M_{j_1,w_1}^{F,v_1}} \sqrt{M_{j_2,v_2}^{R,w_2}} \right\| = \lim_{\alpha \rightarrow \infty} \left\{ \text{Tr} \left( \left[ \sqrt{O} \right]^\alpha \right) \right\}^{1/\alpha} \quad (\text{A8})$$

$$= \lim_{\alpha \rightarrow \infty} \left[ \sum_{r=1}^{d_1} (\Lambda_1^r)^{\alpha/2} \right]^{1/\alpha}. \quad (\text{A9})$$

Only the greatest eigenvalue to survives:  $\left\| \sqrt{M_{j_1,w_1}^{F,v_1}} \sqrt{M_{j_2,v_2}^{R,w_2}} \right\| = \sqrt{\Lambda_1^{\max}}$ . But  $\Lambda_1^{\max}$  is neither a parameter chosen by the experimentalist nor obviously experimentally measurable. Hence bounding the entropies with  $\Lambda_1^{\max}$  is useless.

Probabilities and quasiprobabilities are measurable.  $\text{Tr}(O)$  equals a combination of probabilities and quasiprobabilities. We therefore seek to shift the  $\text{Tr}$  of Eq. (A8) inside the  $[.]^\alpha$  and the  $\sqrt{\cdot}$ . Equivalently, we seek to shift the  $\sum$  of Eq. (A9) inside the  $(.)^{\alpha/2}$ . We do so at the cost of introducing an inequality:

$$\sum_r (\Lambda_1^r)^{\alpha/2} \leq \left( \sum_r \Lambda_1^r \right)^{\alpha/2} \quad (\text{A10})$$

<sup>12</sup> We must prove that  $\left\{ \left( K_{j_2}^{V,v_2} \right)^\dagger \right\}_{j_2}$  defines a quantum channel.  $\left\{ K_{j_2}^{V,v_2} \right\}_{j_2}$  does by definition, so each  $K_{j_2}^{V,v_2}$  maps the input Hilbert space to the output Hilbert space, and  $\sum_{j_2} \left( K_{j_2}^{V,v_2} \right)^\dagger K_{j_2}^{V,v_2} = \mathbb{1}$ . The operator  $K_{j_2}^{V,v_2}$  differs from  $\left( K_{j_2}^{V,v_2} \right)^\dagger$  only by complex conjugation of the coupling  $g_{j_2}^V \in \mathbb{C}$ . Hence  $\sum_{j_2} K_{j_2}^{V,v_2} \left( K_{j_2}^{V,v_2} \right)^\dagger = \mathbb{1}$ , as required of Kraus operators. This mathematical result complements physical intuition:

Suppose that the detector manifests as a qubit. A common interaction rotates the detector's state conditionally on the system's state [36, 41, 139]. Let  $\left\{ K_{j_2}^{V,v_2} \right\}_{j_2}$  follow from a rotation in some fiducial direction.  $\left\{ \left( K_{j_2}^{V,v_2} \right)^\dagger \right\}_{j_2}$  follows from a rotation in the opposite direction. Now, suppose that the detector manifests as a particle in some potential. A common interaction conditionally kicks the detector. If  $\left\{ K_{j_2}^{V,v_2} \right\}_{j_2}$  follows from a kick in one direction,  $\left\{ \left( K_{j_2}^{V,v_2} \right)^\dagger \right\}_{j_2}$  follows from a kick in the opposite.

for all  $\alpha/2 \geq 1$ . This inequality follows from the Schatten  $p$ -norm's monotonicity. The Schatten  $p$ -norm of an operator  $\sigma$  is defined as  $\|\sigma\|_p := \left[ \text{Tr} \left( \sqrt{\sigma^\dagger \sigma}^p \right) \right]^{1/p}$ , for  $p \in [1, \infty)$ . As  $p$  increases, the Schatten norm decreases monotonically:

$$\|\sigma\|_p \leq \|\sigma\|_q \quad \text{if } p \geq q. \quad (\text{A11})$$

Let  $p = \alpha/2$  and  $q = 1$ . Raising each side of Ineq. (A11) to the  $\alpha/2$  power yields Ineq. (A10). Applying Ineq. (A10) to Eq. (A9) bounds the operator norm as

$$\left\| \sqrt{M_{j_1, w_1}^{\text{F}, v_1}} \sqrt{M_{j_2, v_2}^{\text{R}, w_2}} \right\| \leq \sqrt{\text{Tr} \left( \Pi_{w_2}^{W(t)} K_{j_2}^{V, v_2} \left[ K_{j_1}^{V, v_1} \right]^\dagger \Pi_{w_1}^{W(t)} K_{j_1}^{V, v_1} \left[ K_{j_2}^{V, v_2} \right]^\dagger \right)}. \quad (\text{A12})$$

We have invoked the trace's cyclicity and  $\left( \Pi_{w_2}^{W(t)} \right)^2 = \Pi_{w_2}^{W(t)}$ .

Substituting into Eq. (A3) bounds the overlap:

$$c \left( \left\{ M_{j_1, w_1}^{\text{F}, v_1} \right\}, \left\{ M_{j_2, v_2}^{\text{R}, w_2} \right\} \right) \leq \max_{j_1, j_2, w_1, w_2} \left\{ \text{Tr} \left( \Pi_{w_2}^{W(t)} K_{j_2}^{V, v_2} \left[ K_{j_1}^{V, v_1} \right]^\dagger \Pi_{w_1}^{W(t)} K_{j_1}^{V, v_1} \left[ K_{j_2}^{V, v_2} \right]^\dagger \right) \right\}. \quad (\text{A13})$$

We substitute into the trace from Eqs. (13) and (14):

$$\begin{aligned} c \left( \left\{ M_{j_1, w_1}^{\text{F}, v_1} \right\}, \left\{ M_{j_2, v_2}^{\text{R}, w_2} \right\} \right) &\leq \max_{j_1, j_2, w_1, w_2} \left\{ \text{Tr} \left( \Pi_{w_2}^{W(t)} \left[ \sqrt{p_{j_2}^V} \mathbb{1} + g_{j_2}^V \Pi_{v_2}^V \right] \right. \right. \\ &\quad \times \left. \left. \left\{ \sqrt{p_{j_1}^V} \mathbb{1} + [g_{j_1}^V]^* \Pi_{v_1}^V \right\} \Pi_{w_1}^{W(t)} \left[ \sqrt{p_{j_1}^V} \mathbb{1} + g_{j_1}^V \Pi_{v_1}^V \right] \left\{ \sqrt{p_{j_2}^V} \mathbb{1} + [g_{j_2}^V]^* \Pi_{v_1}^V \right\} \right) \right\}. \end{aligned} \quad (\text{A14})$$

Multiplying out yields

$$\begin{aligned} c \left( \left\{ M_{j_1, w_1}^{\text{F}, v_1} \right\}, \left\{ M_{j_2, v_2}^{\text{R}, w_2} \right\} \right) &\leq \max_{j_1, j_2, w_1, w_2} \left\{ p_{j_1}^V p_{j_2}^V \text{Tr} \left( \Pi_{w_2}^W \right) \delta_{w_1 w_2} \right. \\ &\quad + \left[ 2\sqrt{p_{j_1}^V} p_{j_2}^V \text{Re} \left( g_{j_1}^V \right) \text{Tr} \left( \Pi_{w_2}^{W(t)} \Pi_{v_1}^V \right) \delta_{w_1 w_2} + 2p_{j_1}^V \sqrt{p_{j_2}^V} \text{Re} \left( g_{j_2}^V \right) \text{Tr} \left( \Pi_{w_2}^W \Pi_{v_2}^V \right) \delta_{w_1 w_2} \right] \\ &\quad + \left[ p_{j_2}^V |g_{j_1}^V|^2 \text{Tr} \left( \Pi_{w_2}^{W(t)} \Pi_{v_1}^V \Pi_{w_1}^{W(t)} \Pi_{v_1}^V \right) + p_{j_1}^V |g_{j_2}^V|^2 \text{Tr} \left( \Pi_{w_2}^{W(t)} \Pi_{v_2}^V \Pi_{w_1}^{W(t)} \Pi_{v_2}^V \right) \right. \\ &\quad + 2\sqrt{p_{j_1}^V p_{j_2}^V} \text{Re} \left( g_{j_1}^V g_{j_2}^V \text{Tr} \left( \Pi_{w_2}^{W(t)} \Pi_{v_2}^V \Pi_{w_1}^{W(t)} \Pi_{v_1}^V \right) \right) + 2\sqrt{p_{j_1}^V p_{j_2}^V} \text{Re} \left( g_{j_1}^V [g_{j_2}^V]^* \right) \text{Tr} \left( \Pi_{w_2}^{W(t)} \Pi_{v_1}^V \right) \delta_{v_1 v_2} \delta_{w_1 w_2} \\ &\quad + 2\sqrt{p_{j_2}^V} |g_{j_1}^V|^2 \text{Re} \left( g_{j_2}^V \text{Tr} \left( \Pi_{w_2}^{W(t)} \Pi_{v_2}^V \Pi_{w_1}^{W(t)} \Pi_{v_1}^V \right) \right) \delta_{v_1 v_2} \\ &\quad \left. + 2\sqrt{p_{j_1}^V} |g_{j_2}^V|^2 \text{Re} \left( g_{j_1}^V \text{Tr} \left( \Pi_{w_2}^{W(t)} \Pi_{v_2}^V \Pi_{w_1}^{W(t)} \Pi_{v_1}^V \right) \right) \delta_{v_1 v_2} \right] + |g_{j_1}^V|^2 |g_{j_2}^V|^2 \text{Tr} \left( \Pi_{w_2}^{W(t)} \Pi_{v_2}^V \Pi_{w_1}^{W(t)} \Pi_{v_1}^V \right) \delta_{v_1 v_2} \}. \end{aligned} \quad (\text{A15})$$

Six of the traces are instances of  $\tilde{\mathcal{A}}_1$ .

Only the first term is constant in  $g$ . If  $g$  is small, therefore, the maximum obtains where the first term maximizes, where  $w_1 = w_2$ . Hence every RHS term is implicitly evaluated at  $w_1 = w_2$ .

We take the log of each side of Ineq. (A15). The log's monotonicity implies  $\log c \leq \max \{ \log(\dots) \}$ . We negate each side, then shift the negative sign across the max (as negative logs evoke entropies):  $-\log c \geq -\max \{ \log(\dots) \} = \min \{ -\log(\dots) \}$ . With this inequality and with Ineq. (A15), we bound the RHS of Ineq. (A1).

Next, we factor out the  $p_{j_1}^V p_{j_2}^V \text{Tr} \left( \Pi_{w_2}^W \right)$  and invoke the log law for multiplication:  $\min \{ -\log (p_{j_1}^V p_{j_2}^V \text{Tr} \left( \Pi_{w_2}^W \right)) + \log (1 + [\text{terms small in } g]) \}$ . We then Taylor-approximate in the  $g$ 's. The quasiprobability values are assumed to be small enough not to undermine the Taylor approximation. This assumption is reasonable: OTOC quasiprobability values  $> 1$  have not been observed in any of the numerical simulations performed for this paper or for [36]. Moreover, the  $g$ 's can always be weakened enough to offset any largeness of  $\tilde{\mathcal{A}}_1$ .

## Appendix B ANALYTICAL CALCULATIONS FOR THE SPIN-CHAIN EXAMPLE

Let us derive the results in Sec. II 1 2. We calculate the detector probability  $p_{j_\ell}^{\hat{V}} \equiv p_{x_\ell}^{\hat{V}}$ , the weak-measurement Kraus operators  $\hat{K}_{j_\ell}^{\hat{V}, v_\ell} \equiv \hat{K}_{x_\ell}^{\hat{V}, v_\ell}$ , the coupling strengths  $g_{j_\ell}^{\hat{V}} \equiv g_{x_\ell}^{\hat{V}}$ , and the entropies  $H_\alpha$ .

**Detector probability**  $p_{j_\ell}^{\hat{V}} \equiv p_{x_\ell}^{\hat{V}}$ : Consider preparing the detector in  $|D\rangle$ , then measuring  $\hat{x}$ . The measurement has a probability  $p_{x_\ell}^{\hat{V}} L = |\langle x_\ell | D \rangle|^2 L$  of yielding a position within  $L$  of  $x_\ell$ . By Eq. (32),

$$p_{x_\ell}^{\hat{V}} L = \frac{L\Delta}{\sqrt{\pi}\hbar} e^{-\Delta^2(x_\ell)^2/\hbar^2}. \quad (\text{B1})$$

Equation (B1) determines the condition under which the uncertainty bound is nontrivial. The term

$$\min_{x_1, x_2, w_2} \left\{ -\log \left( p_{x_1}^{\hat{V}} p_{x_2}^{\hat{V}} \text{Tr}(\Pi_{w_2}^W) \right) \right\} \quad (\text{B2})$$

dominates the bound (26). The trace equals  $2^{N-1}$ . The bound is positive when  $p_{x_1}^{\hat{V}} p_{x_2}^{\hat{V}} 2^{N-1} \leq 1$ . The min, acting on Eq. (B1), chooses  $x_1 = x_2 = 0$ . We substitute in from Eq. (B1), then solve for  $L\Delta$ :

$$L\Delta \leq \hbar \sqrt{\frac{\pi}{2^{N-1}}}. \quad (\text{B3})$$

Inequality (B3) does not violate Heisenberg's measurement-disturbance uncertainty relation [46]: A finite time separates the  $|D\rangle$  preparation from the  $\hat{x}$  measurement. Yet the  $\hbar$  and  $\frac{1}{\sqrt{2^{N-1}}}$  suggest that meeting the condition might pose practical difficulties. A rough estimate offers hope: Recent many-body experiments featured rubidium atoms cooled to  $\approx 1 \times 10^{-5}$  K [140]. The rubidium atom has a mass of  $m \approx 1 \times 10^{-25}$  kg. Denoting Boltzmann's constant by  $k_B$ , we approximate  $k_B T \approx \frac{p^2}{2m}$ . The momentum  $p \approx \sqrt{2mk_B T} \approx 4 \times 10^{-27}$  kg · m / s stands in for  $\Delta$ . Lengths in periodic arrays can be measured with X-ray diffraction. Precisions of up to  $L \approx 10^{-18}$  m have been achieved with silicon [141, 142]. (Though silicon lattices differ from rubidium arrays, both numbers reflect precision achievable with quantum experiments today.) Substituting into the bound, then rearranging, yields  $N \approx 50$ . Approximately the same number of rubidium atoms formed the quantum simulator in [140].

**Weak-measurement Kraus operators**  $\hat{K}_{j_\ell}^{\hat{V}, v_\ell} \equiv \hat{K}_{x_\ell}^{\hat{V}, v_\ell}$  **and coupling strengths**  $g_{j_\ell}^{\hat{V}} \equiv g_{x_\ell}^{\hat{V}}$ : The Kraus operators have the form (to within a global phase)

$$\langle x_\ell | \hat{V}_{\text{int}} | D \rangle = \langle x_\ell | D \rangle \exp \left( -\frac{i}{\hbar} \tilde{g} [x_\ell - x_0] \hat{\Pi}_{v_\ell}^{\hat{V}} \right). \quad (\text{B4})$$

We redefine the Kraus operators such that the coefficient is real:

$$\hat{K}_{x_\ell}^{\hat{V}, v_\ell} := |\langle x_\ell | D \rangle| \exp \left( -\frac{i}{\hbar} \tilde{g} [x_\ell - x_0] \hat{\Pi}_{v_\ell}^{\hat{V}} \right) \quad (\text{B5})$$

$$= \sqrt{p_{x_\ell}^{\hat{V}}} \hat{\mathbb{1}} + g_{x_\ell}^{\hat{V}} \hat{\Pi}_{v_\ell}^{\hat{V}}. \quad (\text{B6})$$

The outcome-dependent coupling is

$$g_{x_\ell}^{\hat{V}} = \sqrt{p_{x_\ell}^{\hat{V}}} \left( e^{-\frac{i}{\hbar} \tilde{g}(x_\ell - x_0)} - 1 \right). \quad (\text{B7})$$

We chose  $\Delta = 0.1$ , which (with  $L = 0.1$ ,  $\hbar = 1$ , and  $N = 8$ ) satisfies Ineq. (B3).

### Appendix C CHOICE OF $v_1 = -v_2$ IN THE SPIN-CHAIN EXAMPLE

Equation (60) on p. 15 of [36] motivates our choice.  $\tilde{\mathcal{A}}_1(v_1, w_1, v_2, w_2)$  appears, there, as a combination of correlators of  $V$  and  $W(t)$ . Let us set  $w_1 = w_2$  and replace  $\rho$  with  $\hat{\mathbb{1}}$ . We recall that  $w_\ell, v_m = \pm 1$ , that the Pauli operators' traces vanish, and that the Pauli operators square to  $\hat{\mathbb{1}}$ . The expression simplifies:

$$\tilde{\mathcal{A}}_1(v_1, w_2, v_2, w_2) = \frac{1}{16} [2 + v_1 v_2 + 2w_2(v_1 + v_2) \langle VW(t) \rangle + (w_2)^2 v_1 v_2 F(t)]. \quad (\text{C1})$$

Let us analyze the expression piecemeal. First, the  $\langle VW(t) \rangle \approx 0$  at early times, because the influence from  $V$  has not reached  $W(t)$ . Random-matrix-theory cancellations suppress  $\langle VW(t) \rangle$  at late times. Second, the OTOC begins at  $F(t \approx 0) \approx 1$  and drops to  $F(t \geq t_*) \approx 0$ . Third, suppose that  $v_1 = -v_2$ .

Combining these three behaviors, we infer the behavior of the RHS of Eq. (C1). The first three terms sum to  $\approx 1$ . The final term rises from  $\approx -1$  to  $\approx 0$ . Therefore,  $\tilde{\mathcal{A}}_1(v_1, w_2, -v_1, w_2)$  rises from  $\approx 0$  to  $\approx \frac{1}{16}$ .

This rise strengthens the bound  $f(v_1, v_2 = -v_1)$ :  $\tilde{\mathcal{A}}_1(v_1, w_2, -v_1, w_2)$  contributes to the bound through the term

$$\frac{-2}{\ln 2 \operatorname{Tr}(\Pi_{w_2}^W) \sqrt{p_{j_1}^V p_{j_2}^V}} \operatorname{Re} \left( g_{j_1}^V g_{j_2}^V \tilde{\mathcal{A}}_1(v_1, w_2, -v_1, w_2) \right) \quad (\text{C2})$$

in line (30). We have chosen for the couplings to have large imaginary parts, so  $g_{j_1}^V g_{j_2}^V$  is dominated by  $-\tilde{g}^2 < 0$ . The quasiprobability is real for all arguments [36, p. 24]. Around  $t = t_*$ , therefore, (C2) rises from  $\approx 0$  to  $\approx \frac{-\tilde{g}^2}{\ln(2) 2^{N+2} \sqrt{p_{j_1}^V p_{j_2}^V}}$ , tightening the bound.

In summary, the final  $\tilde{\mathcal{A}}_1$  value in (30) points to  $v_1 = -v_2$  as a condition under which the uncertainty bound is relatively tight. We arbitrarily chose  $v_1 = 1$ .

Why should the first two  $\tilde{\mathcal{A}}_1$  terms in (30) not guide our choice of  $(v_1, v_2)$ ? These terms influence the bound through

$$\frac{-1}{\ln 2 \operatorname{Tr}(\Pi_{w_2}^W)} \left[ \frac{|g_{j_1}^V|^2}{p_{j_1}^V} \tilde{\mathcal{A}}_1(v_1, w_1, v_1, w_2) + \frac{|g_{j_2}^V|^2}{p_{j_2}^V} \tilde{\mathcal{A}}_1(v_2, w_1, v_2, w_2) \right]. \quad (\text{C3})$$

By Eq. (C1),  $\tilde{\mathcal{A}}_1(v_1, w_1, v_1, w_2) = \tilde{\mathcal{A}}_1(v_2, w_1, v_2, w_2) = \frac{1}{16} [3 + 4w_2 \langle VW(t) \rangle + F(t)]$ . As argued earlier,  $\langle VW(t) \rangle$  is small at early and late times. Hence  $\tilde{\mathcal{A}}_1(v, w_1, v, w_2) \geq 0$  for all  $v = \pm 1$ . Hence (C3) is expected to be negative, loosening the bound, regardless of our choices of  $v_1$  and  $v_2$ .

## Appendix D CALCULATIONS: QUBIT EXAMPLE FOR THE WEAK-VALUE UNCERTAINTY RELATION

$A$  can be weakly measured as follows. The detector is prepared in the state  $|x+\rangle$ . A  $z$ -controlled  $y$  conditions a rotation of the detector's state on the system's state. The interaction Hamiltonian  $H_{\text{int}} = \tilde{g} (\sigma_d^y \otimes \sigma_s^z)$  generates the unitary

$$V_{\text{int}} = \exp(-i\tilde{g} [\sigma_d^y \otimes \sigma_s^z]) \quad (\text{D1})$$

$$= \cos(\tilde{g}) \mathbb{1} - i \sin(\tilde{g}) (\sigma_d^y \otimes \sigma_s^z). \quad (\text{D2})$$

The detector's  $\sigma_d^y$  is measured strongly, yielding the outcome  $j = y_d = \pm 1$ .

We can begin assembling the ingredients in Ineq. (52). The coupling-free probabilities  $p_j^A = p_{y_d}^Y = |\langle y_d | x+ \rangle|^2 = \frac{1}{2}$  for  $y_d = \pm 1$ . Next, we calculate the weak-measurement Kraus operators  $K_j^Y$  and the outcome-dependent couplings  $g_j^Y$ .

En route to  $K_j^Y \equiv K_{y_d}^Y$ , we define the physically equivalent

$$\tilde{K}_{y_d}^A = \langle y_d | V_{\text{int}} | x+ \rangle = \cos(\tilde{g}) \langle y_d | x+ \rangle \mathbb{1} - i \sin(\tilde{g}) \langle y_d | \sigma_d^y | x+ \rangle \sigma_s^z. \quad (\text{D3})$$

We remove a global phase:

$$K_j^A = \frac{|\langle y_d | x+ \rangle|}{\langle y_d | x+ \rangle} \tilde{K}_{y_d}^A \quad (\text{D4})$$

$$= \cos(\tilde{g}) |\langle y_d | x+ \rangle| \mathbb{1} - i \sin(\tilde{g}) \frac{\langle y_d | \sigma_d^y | x+ \rangle}{\langle y_d | x+ \rangle} |\langle y_d | x+ \rangle| \sigma_s^z. \quad (\text{D5})$$

To first order in  $\tilde{g}$ ,

$$K_{y_d}^Y = \sqrt{p_{y_d}^Y} \mathbb{1} + g_{y_d}^Y \sigma_s^z + O(\tilde{g}^2). \quad (\text{D6})$$

The outcome-dependent coupling has the form

$$g_j^A \equiv g_{y_d}^Y := -i\tilde{g} \langle y_d | \sigma^y | x+ \rangle \frac{|\langle y_d | x+ \rangle|}{\langle y_d | x+ \rangle} = \frac{-y_d i}{\sqrt{2}} \tilde{g}. \quad (\text{D7})$$

The weak value has the form  $A_{\text{wk}}(z_s, x_s) = \langle x_s | \sigma_s^y | z_s \rangle / \langle x_s | z_s \rangle = x_s z_s i$ . The nonreality is nonclassical [88]. Let us calculate the bound (53).  $f_{\text{wk}}$  contains a factor  $\text{Re}(g_j^A A_{\text{wk}}(i, f)) = \text{Re}(g_{y_d}^Y A_{\text{wk}}(z_s, x_s)) = y_d x_s z_s \tilde{g} / \sqrt{2}$ . When this factor maximizes at  $\frac{|\tilde{g}|}{\sqrt{2}}$ , the minimum in  $f_{\text{wk}}$  is attained. The probability  $\text{Tr}(\Pi_f^F \Pi_i^T) = |\langle x_s | z_s \rangle|^2 = \frac{1}{2}$  for all  $x_s, z_s = \pm 1$ . Substituting into Eq. (53) yields

$$\min_{z_s, y_d, x_s} \left\{ -\log(p_{y_d}^Y |\langle x_s | z_s \rangle|^2) - \frac{2}{\ln 2 \sqrt{p_{y_d}^Y}} \text{Re}(g_{y_d}^Y A_{\text{wk}}(z_s, x_s)) + O(\tilde{g}^2) \right\} = 2 - \frac{2}{\ln 2} |\tilde{g}| + O(\tilde{g}^2). \quad (\text{D8})$$

Having evaluated the RHS of Ineq. (52), we turn to the LHS. We calculate the POVM probabilities, then their entropies.  $\rho$  denotes an arbitrary system state, exemplified by  $|z+\rangle$ .

POVM II consists of a strong  $\mathcal{I} = \sigma_s^z$  measurement. The possible outcomes  $z_s$  have probabilities  $q_{z_s}^{\text{II}} = \langle z_s | \rho | z_s \rangle$  of obtaining. If  $\rho = |z+\rangle\langle z+|$ , then  $q_{z_s=1}^{\text{II}} = 1$ , and  $q_{z_s=-1}^{\text{II}} = 0$ . The max entropy is  $H_{\text{max}}(\{q_{z_s}^{\text{II}}\}) = \log 1 = 0$ . Smoothing cannot change this value.

POVM I consists of a weak  $A = \sigma_s^y$  measurement followed by a strong  $F = \sigma_s^x$  measurement. The possible outcome tuples  $(y_d, x_s)$  correspond to the probabilities  $q_{y_d, x_s}^{\mathcal{I}} = \langle x_s | K_{y_d}^Y \rho (K_{y_d}^Y)^\dagger | x_s \rangle$ . We substitute in, then multiply out:

$$q_{y_d, x_s}^{\mathcal{I}} = p_{y_d}^Y \langle x_s | \rho | x_s \rangle + \sqrt{p_{y_d}^Y} \left[ g_{y_d}^Y \langle x_s | \sigma^z \rho | x_s \rangle + (g_{y_d}^Y)^* \langle x_s | \rho \sigma^z | x_s \rangle \right] + O(\tilde{g}^2). \quad (\text{D9})$$

If  $\rho = |z+\rangle\langle z+|$ , the distribution is uniform:  $q_{y_d, x_s}^{\mathcal{I}} = \frac{1}{4} + O(\tilde{g}^2)$  for all  $y_d, x_s = \pm 1$ . Hence  $H_{\text{min}}(\{q_{y_d, x_s}^{\mathcal{I}}\}) = 2.00 + O(\tilde{g}^2)$ . Nor can smoothing alter this value.

## REFERENCES

- [1] H. Everett, *Reviews of Modern Physics* **29**, 454 (1957).
- [2] I. I. Hirschman, *American Journal of Mathematics* **79**, 152 (1957).
- [3] W. Beckner, *Annals of Mathematics* **102**, 159 (1975).
- [4] I. Bialynicki-Birula and J. Mycielski, *Communications in Mathematical Physics* **44**, 129 (1975).
- [5] D. Deutsch, *Phys. Rev. Lett.* **50**, 631 (1983).
- [6] K. Kraus, *Phys. Rev. D* **35**, 3070 (1987).
- [7] H. Maassen and J. B. M. Uffink, *Phys. Rev. Lett.* **60**, 1103 (1988).
- [8] G. Ghirardi, L. Marinatto, and R. Romano, *Physics Letters A* **317**, 32 (2003), quant-ph/0310120.
- [9] M. Christandl and A. Winter, *IEEE Transactions on Information Theory* **51**, 3159 (2005).
- [10] J. I. de Vicente and J. Sánchez-Ruiz, *Phys. Rev. A* **77**, 042110 (2008), 0709.1438.
- [11] J. M. Renes and J.-C. Boileau, *Physical Review Letters* **103**, 020402 (2009).
- [12] M. Berta, M. Christandl, R. Colbeck, J. M. Renes, and R. Renner, *Nature Physics* **6**, 659 (2010), 0909.0950.
- [13] P. J. Coles, R. Colbeck, L. Yu, and M. Zwolak, *Physical Review Letters* **108**, 210405 (2012), 1112.0543.
- [14] M. Tomamichel, *A Framework for Non-Asymptotic Quantum Information Theory*, PhD thesis, ETH Zürich, 2012.
- [15] P. J. Coles, M. Berta, M. Tomamichel, and S. Wehner, *Rev. Mod. Phys.* **89**, 015002 (2017).
- [16] S. Wehner and A. Winter, *New Journal of Physics* **12**, 025009 (2010).
- [17] A. Larkin and Y. N. Ovchinnikov, *Soviet Journal of Experimental and Theoretical Physics* **28** (1969).
- [18] N. Lashkari, D. Stanford, M. Hastings, T. Osborne, and P. Hayden, *Journal of High Energy Physics* **2013**, 22 (2013).
- [19] A. Kitaev, A simple model of quantum holography, KITP strings seminar and Entanglement 2015 program, 2015.
- [20] S. H. Shenker and D. Stanford, *Journal of High Energy Physics* **3**, 67 (2014).
- [21] S. H. Shenker and D. Stanford, *Journal of High Energy Physics* **12**, 46 (2014).
- [22] D. A. Roberts, D. Stanford, and L. Susskind, *Journal of High Energy Physics* **3**, 51 (2015).
- [23] D. A. Roberts and D. Stanford, *Physical Review Letters* **115**, 131603 (2015).
- [24] J. Maldacena, S. H. Shenker, and D. Stanford, *ArXiv e-prints* (2015), 1503.01409.
- [25] F. M. Haehl, R. Loganayagam, and M. Rangamani, *Journal of High Energy Physics* **2017**, 69 (2017).
- [26] P. Hosur, X.-L. Qi, D. A. Roberts, and B. Yoshida, *Journal of High Energy Physics* **2**, 4 (2016), 1511.04021.
- [27] A. Bohrdt, C. B. Mendl, M. Endres, and M. Knap, *New Journal of Physics* **19**, 063001 (2017).
- [28] J. Maldacena and D. Stanford, *Phys. Rev. D* **94**, 106002 (2016).
- [29] I. L. Aleiner, L. Faoro, and L. B. Ioffe, *Annals of Physics* **375**, 378 (2016).
- [30] D. A. Roberts and B. Swingle, *Phys. Rev. Lett.* **117**, 091602 (2016).
- [31] Y. Huang, Y.-L. Zhang, and X. Chen, *Annalen der Physik* **529**, 1600318 (2017), <https://onlinelibrary.wiley.com/doi/pdf/10.1002/andp.201600318>.
- [32] B. Swingle and D. Chowdhury, *Phys. Rev. B* **95**, 060201 (2017).
- [33] R. Fan, P. Zhang, H. Shen, and H. Zhai, *Science Bulletin* **62**, 707 (2017).
- [34] R.-Q. He and Z.-Y. Lu, *Phys. Rev. B* **95**, 054201 (2017).

- [35] N. Yunger Halpern, Phys. Rev. A **95**, 012120 (2017).
- [36] N. Yunger Halpern, B. Swingle, and J. Dressel, Phys. Rev. A **97**, 042105 (2018).
- [37] J. R. González Alonso, N. Yunger Halpern, and J. Dressel, Phys. Rev. Lett. **122**, 040404 (2019).
- [38] D. A. Roberts and B. Yoshida, Journal of High Energy Physics **2017**, 121 (2017).
- [39] F. M. Haehl, R. Loganayagam, P. Narayan, and M. Rangamani, ArXiv e-prints (2017), 1701.02820.
- [40] F. M. Haehl, R. Loganayagam, P. Narayan, A. A. Nizami, and M. Rangamani, Journal of High Energy Physics **2017**, 154 (2017).
- [41] J. Dressel, J. R. González Alonso, M. Waegell, and N. Yunger Halpern, Phys. Rev. A **98**, 012132 (2018).
- [42] F. M. Haehl and M. Rozali, Phys. Rev. Lett. **120**, 121601 (2018).
- [43] B. Tamir and E. Cohen, Quanta **2**, 7 (2013).
- [44] Y. Aharonov, D. Z. Albert, and L. Vaidman, Phys. Rev. Lett. **60**, 1351 (1988).
- [45] J. Dressel, M. Malik, F. M. Miatto, A. N. Jordan, and R. W. Boyd, Rev. Mod. Phys. **86**, 307 (2014).
- [46] W. Heisenberg, Zeitschrift für Physik **43**, 172 (1927).
- [47] E. H. Kennard, Zeitschrift für Physik **44**, 326 (1927).
- [48] H. P. Robertson, Phys. Rev. **34**, 163 (1929).
- [49] C. E. Shannon, The Bell System Technical Journal **27**, 379 (1948).
- [50] M. A. Nielsen and I. L. Chuang, *Quantum Computation and Quantum Information* (Cambridge University Press, 2010).
- [51] M. Tomamichel, *Quantum Information Processing with Finite Resources - Mathematical Foundations* (Springer, 2016).
- [52] M. M. Wilde, *Quantum Information Theory*, 2 ed. (Cambridge University Press, 2017).
- [53] M. Gärttner *et al.*, Nature Physics **13**, 781 (2017), Article.
- [54] S. Sachdev and J. Ye, Phys. Rev. Lett. **70**, 3339 (1993).
- [55] J. Polchinski and V. Rosenhaus, Journal of High Energy Physics **4**, 1 (2016), 1601.06768.
- [56] W. Brown and O. Fawzi, ArXiv e-prints (2012), 1210.6644.
- [57] D. Gross, *Computational Power of Quantum Many-Body States and Some Results on Discrete Phase Spaces*, PhD thesis, Imperial College London, 2005.
- [58] R. W. Spekkens, Phys. Rev. Lett. **101**, 020401 (2008).
- [59] V. Veitch, C. Ferrie, D. Gross, and J. Emerson, New Journal of Physics **14**, 113011 (2012).
- [60] M. Howard, J. Wallman, V. Veitch, and J. Emerson, Nature **510**, 351 (2014).
- [61] M. Krishna and K. Parthasarathy, eprint arXiv:quant-ph/0110025 (2001), quant-ph/0110025.
- [62] J. Preskill, Quantum computation: Ch. 3: Foundations of quantum theory ii: Measurement and evolution, Lecture notes, 2015.
- [63] R. Bhatia, *Matrix analysis* (Springer, New York, 1997).
- [64] R. Renner, *Security of Quantum Key Distribution*, PhD thesis, PhD Thesis, 2005, 2005.
- [65] L. del Río, J. Åberg, R. Renner, O. Dahlsten, and V. Vedral, Nature **474**, 61 (2011).
- [66] M. Berta, *Quantum Side Information: Uncertainty Relations, Extractors, Channel Simulations*, PhD thesis, ETH Zürich, 2013.
- [67] F. Leditzky, *Relative entropies and their use in quantum information theory*, PhD thesis, U. of Cambridge, 2016.
- [68] F. Leditzky, M. M. Wilde, and N. Datta, Journal of Mathematical Physics **57**, 082202 (2016), <https://doi.org/10.1063/1.4960099>.
- [69] P. Faist and R. Renner, Phys. Rev. X **8**, 021011 (2018).
- [70] A. E. Rastegin, ArXiv e-prints (2008), 0805.1777.
- [71] M. Campisi and J. Goold, Phys. Rev. E **95**, 062127 (2017).
- [72] B. Swingle and N. Yunger Halpern, Phys. Rev. A **97**, 062113 (2018).
- [73] X. Chen, T. Zhou, and C. Xu, ArXiv e-prints (2017), 1712.06054.
- [74] G. de Lange *et al.*, Phys. Rev. Lett. **112**, 080501 (2014).
- [75] J. S. Lundeen, B. Sutherland, A. Patel, C. Stewart, and C. Bamber, Nature **474**, 188 (2011).
- [76] J. Li *et al.*, Phys. Rev. X **7**, 031011 (2017).
- [77] Simulation code and data.
- [78] J. G. Kirkwood, Physical Review **44**, 31 (1933).
- [79] P. A. M. Dirac, Rev. Mod. Phys. **17**, 195 (1945).
- [80] C. Ferrie and J. Combes, Phys. Rev. Lett. **113**, 120404 (2014).
- [81] L. Vaidman, ArXiv e-prints (2014), 1409.5386.
- [82] E. Cohen, ArXiv e-prints (2014), 1409.8555.
- [83] Y. Aharonov and D. Rohrlich, ArXiv e-prints (2014), 1410.0381.
- [84] D. Sokolovski, ArXiv e-prints (2014), 1410.0570.
- [85] A. Brodutch, Phys. Rev. Lett. **114**, 118901 (2015).
- [86] C. Ferrie and J. Combes, Phys. Rev. Lett. **114**, 118902 (2015).
- [87] J. Dressel, Phys. Rev. A **91**, 032116 (2015).
- [88] J. Dressel and A. N. Jordan, Phys. Rev. A **85**, 012107 (2012).
- [89] J. S. Lundeen and C. Bamber, Phys. Rev. Lett. **108**, 070402 (2012).
- [90] L. M. Johansen, Phys. Lett. A **329**, 184 (2004).
- [91] M. J. W. Hall, Phys. Rev. A **64**, 052103 (2001).
- [92] M. J. W. Hall, Phys. Rev. A **69**, 052113 (2004).
- [93] M. J. W. Hall, A. K. Pati, and J. Wu, Phys. Rev. A **93**, 052118 (2016).

[94] P. Hayden and J. Preskill, *Journal of High Energy Physics* **2007**, 120 (2007).

[95] B. Swingle, *Phys. Rev. D* **86**, 065007 (2012).

[96] D. Harlow and P. Hayden, *Journal of High Energy Physics* **2013**, 85 (2013).

[97] F. Pastawski, B. Yoshida, D. Harlow, and J. Preskill, *Journal of High Energy Physics* **2015**, 149 (2015).

[98] N. Bao *et al.*, *Journal of High Energy Physics* **2015**, 130 (2015).

[99] A. R. Brown and L. Susskind, *Phys. Rev. D* **97**, 086015 (2018).

[100] K.-W. Bong *et al.*, *Phys. Rev. Lett.* **120**, 230402 (2018).

[101] Y. Sekino and L. Susskind, *Journal of High Energy Physics* **2008**, 065 (2008).

[102] K. I. Babenko, *Izv. Akad. Nauk SSSR Ser. Mat.* **25**, 531 (1961).

[103] X. Guanlei, W. Xiaotong, and X. Xiaogang, *Signal Processing* **89**, 2692 (2009), Special Section: Visual Information Analysis for Security.

[104] Y. Huang, *Phys. Rev. A* **83**, 052124 (2011).

[105] I. Bialynicki-Birula and L. Rudnicki, *Entropic Uncertainty Relations in Quantum Physics* (Springer Netherlands, Dordrecht, 2011), pp. 1–34.

[106] I. Bialynicki-Birula, *Phys. Rev. A* **74**, 052101 (2006).

[107] B. Swingle, G. Bentsen, M. Schleier-Smith, and P. Hayden, *Phys. Rev. A* **94**, 040302 (2016).

[108] N. Y. Yao *et al.*, ArXiv e-prints (2016), 1607.01801.

[109] G. Zhu, M. Hafezi, and T. Grover, ArXiv e-prints (2016), 1607.00079.

[110] N. Tsuji, P. Werner, and M. Ueda, *Phys. Rev. A* **95**, 011601 (2017).

[111] N. Tsuji, T. Shitara, and M. Ueda, *Phys. Rev. E* **97**, 012101 (2018).

[112] K. X. Wei, C. Ramanathan, and P. Cappellaro, ArXiv e-prints (2016), 1612.05249.

[113] E. J. Meier, J. Ang’ong’aa, F. A. An, and B. Gadway, ArXiv e-prints (2017), 1705.06714.

[114] N. W. M. Ritchie, J. G. Story, and R. G. Hulet, *Phys. Rev. Lett.* **66**, 1107 (1991).

[115] G. J. Pryde, J. L. O’Brien, A. G. White, T. C. Ralph, and H. M. Wiseman, *Phys. Rev. Lett.* **94**, 220405 (2005).

[116] V. Bollen, Y. M. Sua, and K. F. Lee, *Phys. Rev. A* **81**, 063826 (2010).

[117] J. P. Groen *et al.*, *Phys. Rev. Lett.* **111**, 090506 (2013).

[118] C. Bamber and J. S. Lundeen, *Phys. Rev. Lett.* **112**, 070405 (2014).

[119] M. Mirhosseini, O. S. Magaña Loaiza, S. M. Hashemi Rafsanjani, and R. W. Boyd, *Phys. Rev. Lett.* **113**, 090402 (2014).

[120] G. A. Smith, S. Chaudhury, A. Silberfarb, I. H. Deutsch, and P. S. Jessen, *Phys. Rev. Lett.* **93**, 163602 (2004).

[121] S. Hacohen-Gourgy *et al.*, *Nature* **538**, 491 (2016).

[122] T. C. White *et al.*, *npj Quantum Information* **2**, 15022 (2016).

[123] J.-S. Chen *et al.*, ArXiv e-prints (2018), 1805.02235.

[124] G. Sulyok *et al.*, *Phys. Rev. Lett.* **115**, 030401 (2015).

[125] M. Berta, S. Wehner, and M. M. Wilde, *New Journal of Physics* **18**, 073004 (2016).

[126] J. Xing *et al.*, *Scientific Reports* **7**, 2563 (2017).

[127] L. Xiao *et al.*, *Opt. Express* **25**, 17904 (2017).

[128] F. Piacentini *et al.*, *Phys. Rev. Lett.* **117**, 170402 (2016).

[129] Y. Suzuki, M. Iinuma, and H. F. Hofmann, *New Journal of Physics* **18**, 103045 (2016).

[130] G. S. Thekkadath *et al.*, *Phys. Rev. Lett.* **117**, 120401 (2016).

[131] B. Swingle, Quantum many-body systems and quantum gravity, Boulder School for Condensed Matter and Materials Physics, 2018, Lecture notes.

[132] E. F. Galvão, *Phys. Rev. A* **71**, 042302 (2005).

[133] N. Delfosse, P. Allard Guerin, J. Bian, and R. Raussendorf, *Phys. Rev. X* **5**, 021003 (2015).

[134] A. E. Rastegin, ArXiv e-prints (2008), 0807.2691.

[135] M. Tomamichel, C. C. W. Lim, N. Gisin, and R. Renner, *Nature Communications* **3**, 634 (2012), Article.

[136] L. P. Thinh, L. Sheridan, and V. Scarani, *International Journal of Quantum Information* **10**, 1250035 (2012), <https://www.worldscientific.com/doi/pdf/10.1142/S0219749912500359>.

[137] M. Berta, F. Furrer, and V. B. Scholz, *Journal of Mathematical Physics* **57**, 015213 (2016), <https://doi.org/10.1063/1.4936405>.

[138] P. J. Coles and M. Piani, *Phys. Rev. A* **89**, 022112 (2014).

[139] J. Dressel, T. A. Brun, and A. N. Korotkov, *Phys. Rev. A* **90**, 032302 (2014).

[140] H. Bernien *et al.*, *Nature* **551**, 579 (2017), Article.

[141] P. J. Mohr, B. N. Taylor, and D. B. Newell, *Rev. Mod. Phys.* **84**, 1527 (2012).

[142] E. Massa, G. Mana, U. Kuetgens, and L. Ferroglio, *Metrologia* **48**, S37 (2011).